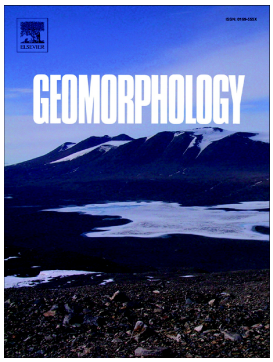

Contaminated sediment flux from eroding abandoned historical metal mines: Spatial and temporal variability in geomorphological drivers

Mark Kincey, Jeff Warburton, Paul Brewer

PII: S0169-555X(18)30284-8
DOI: doi:10.1016/j.geomorph.2018.07.026
Reference: GEOMOR 6463

To appear in: *Geomorphology*

Received date: 15 March 2018
Revised date: 27 July 2018
Accepted date: 28 July 2018

Please cite this article as: Mark Kincey, Jeff Warburton, Paul Brewer , Contaminated sediment flux from eroding abandoned historical metal mines: Spatial and temporal variability in geomorphological drivers. Geomor (2018), doi:10.1016/j.geomorph.2018.07.026

Contaminated sediment flux from eroding abandoned historical metal mines: Spatial and temporal variability in geomorphological drivers

Mark Kincey[a*], Jeff Warburton[a], and Paul Brewer[b]

[a] Department of Geography, Durham University, South Road, Durham, UK

[b] Department of Geography and Earth Sciences, Aberystwyth University, Aberystwyth, UK

Abstract

Abandoned historical metal mines represent significant long-term sediment source locations contributing highly contaminated anthropogenic legacy sediments to river systems. Despite this, our understanding of spatial and temporal variability in the rates and geomorphological drivers of specific contaminated sediment source locations across abandoned mines remains poorly constrained. In this study, sediment flux from two abandoned historical lead mines in the North Pennines, UK, was monitored over an 18 month period using repeat terrestrial laser scanning, enabling the spatial and temporal significance of several common geomorphological processes to be quantified for the first time. A novel contaminated sediment budget approach is used to integrate topographical change data with a pXRF survey of surface sediment metal concentrations. Approximately 434 t (289 t a^{-1}) of eroded sediment entered the stream from a source area of 0.023 km^2. The majority of the erosion was driven by two dominant processes, with gullying accounting for 60% and bank erosion contributing 30%. Redeposition of eroded material within the survey area was minimal (3%), indicating very high levels of coupling between source locations and the stream network and the export of the vast majority of eroded sediments (97%) from the mined area. Rates for all erosive processes were highly episodic and primarily driven by high magnitude, low frequency storm events. Metal concentrations in surface sediments exhibited considerable spatial variability, with notable hotspots around the former ore processing areas and on the tailings heaps. However, 84% of all sediments sampled were in excess of available soil guideline values for Pb and 65% in excess of equivalent guideline values for Zn, indicating that abandoned mine sites still have the potential to be significant sources of contaminant metals and pose a risk to the wider environment. In total, an estimated 4.59 t of Pb and 2.14 t of Zn entered the stream network in a sediment-associated form during the 18 month monitoring period. Although these overall contaminated sediment inputs are high, they are restricted to particular geomorphological processes, are spatially variable in terms of the magnitude of specific source locations, and are delivered in fairly discrete events. This

provides invaluable information for the future management of other abandoned mines and targeted mitigation of their potential legacy effects.

Keywords:

mining contamination; historical metal mining; pXRF; laser scanning

*Correspondence to: Mark Kincey, Department of Geography, Durham University, Durham, DH1 3LE

Email: m.e.kincey@durham.ac.uk

1. Introduction

River catchments impacted by historical metal mining are often highly contaminated, leading to a significant and persistent legacy affecting sediment and water quality (Macklin et al., 2006; Mayes et al., 2010; Luís et al., 2011). Studies worldwide have demonstrated that fluvial systems in former mining areas are frequently still adjusting to historical disturbances related to the influx of large volumes of mine waste (Knighton, 1989; Singer et al., 2013) and typically still contain abnormally high levels of metals at abandoned mine source locations and stored in catchment wide floodplain sediments (Clement et al., 2017; Pavlowsky et al., 2017). In a European context, the Water Framework Directive (WFD) has established clear ecological and chemical water quality target guidelines that have included consideration of pollution caused by abandoned mining operations (European Commission, 2000). However, the focus of such schemes has primarily been on monitoring point source contaminant flux, such as waters draining directly out of mine adits. In contrast, regulatory attention given to more diffuse sources of pollution, and in particular sediment-borne contaminants, has until recently been lacking (Macklin et al., 2006). This is despite the recognition that ~90% of metal contaminants in former mining catchments are commonly sediment-associated rather than in an aqueous form (Hudson-Edwards et al., 2008).

The issue of defining contaminant sources within river catchments as either point or diffuse is dependent on the scale of investigation. For example, at the scale of an entire catchment, abandoned mines would typically be considered as point source locations for contaminated sediments. However, within the context of an individual mine the precise locations of the pollutant inputs will vary spatially owing to the arrangement of former mine workings (levels, waste heaps, etc.), the physical characteristics of the land surface and the distribution of processes driving topographic change. Unlike point sources, such as adit outflows, the spatial location of these sediment sources also changes through time as the condition and stability of the surface is altered and the dominance of different geomorphological processes varies. This spatial and temporal variation means that, at least at the intrasite scale, contaminated sediment inputs are therefore more accurately defined as dispersed in nature rather than as discrete point sources. These dispersed sources share a number of characteristics with more ‘classic’ diffuse sources (e.g., floodplain deposits), including spatial and temporal variability in metal concentrations and the potential for reworking and redistribution of contaminated sediments (Hudson-Edwards et al., 2008).

The hydrological conditions under which point and diffuse contaminant sources dominate are characteristically different. Although point source mine water discharges dominate stream metal loadings during low flows, diffuse inputs are particularly significant during high flow events, when metal-rich sediments are susceptible to entrainment and transport (Mayes et al., 2008; Byrne et al., 2013; Foulds et al., 2014). Diffuse contamination from mining includes direct input of polluted groundwater to surface waters via the hyporheic zone, runoff from mine wastes, and mobilisation of metal-rich floodplain sediments (Dennis et al., 2009; Palumbo-Roe et al., 2012). Owing to their diffuse nature, quantifying such inputs can be problematic, with most studies estimating diffuse source contributions using the residual from mass balance calculations based on measured point source water inputs and stream loadings (Mayes et al., 2008; Mighanetara et al., 2009; Banks and Palumbo-Roe, 2010). Such approaches provide useful approximations of the scale and general location of diffuse inputs but specific details on metal delivery mechanisms to fluvial environments are usually only inferred, limiting their value to practitioners involved in the management or remediation of formerly mined catchments.

The two main sources of diffuse sediment (particulate) contaminants are direct erosion and entrainment of in situ metal-rich mine sediments (e.g., waste heaps) and the remobilisation of previously deposited channel or floodplain sediments (Gozzard et al., 2011). The long-term wider catchment-scale remobilisation and redistribution of mine sediments has received considerable attention by the scientific community for several decades (Lewin et al., 1977; Miller, 1997; Dennis et al., 2003; Clement et al., 2017). Underpinning much of this research has been the recognition that understanding the fluvial geomorphology of a catchment is fundamental to being able to predict the distribution, magnitude, and residence time of associated metal contamination (Brewer et al., 2003; Macklin et al., 2006; Hudson-Edwards et al., 2008; Dennis et al., 2009). In contrast, comparable recent research into the initial mobilisation of in situ sediments directly from abandoned mine source locations has been noticeably lacking despite its significance for a range of other related disciplines such as archaeology (Kincey et al., 2017) and ecology (Batty, 2005).

The importance of in situ mine waste deposits as source locations for contaminated sediments is reflected in policy documents at national (Environment Agency, 2007) and European levels (e.g., the EU Mine Waste Directive, European Commission, 2006). Internationally, even in countries where solid mining waste is not a specifically regulated waste, such as the United States, research into the appropriate management of legacy

mine sites is still seen as a central priority (ITRC (Interstate Technology & Regulatory Council), 2008). However, actually translating knowledge of mine waste site locations and characteristics into an understanding of specific sediment contaminant sources is problematic. In the UK, a recent national assessment of metal mine pollution focused primarily on water quality data, with associated information regarding diffuse sediment contaminants being largely qualitative in nature (Mayes et al., 2009). Where comparable national assessments of sediment-related diffuse pollution have been attempted, these have by necessity been restricted to the use of a relatively simplistic classification of risk based on the mapping of waste deposits and broad topographic characteristics (Turner et al., 2011; Mayes et al., 2015). Local site-scale appraisals of diffuse inputs of contaminated sediments have been undertaken (Forth, 1999), but these have generally tended to either involve qualitative descriptions of visually identified sediment transfer processes (Wray, 1998) or to focus on large-scale catastrophic events, such as tailings dam failures (Macklin et al., 2003; Kossoff et al., 2014). However, the baseline understanding generated through such local-scale assessments is fundamental to being able to develop a comprehensive and accurate understanding of the drivers of surface change and contaminated sediment flux at abandoned mines. Without this detailed process-based knowledge, the validity of broader regional or national assessments cannot be properly evaluated and our ability to introduce effective management schemes or policies remains restricted.

Although not primarily focused on contaminant flux, numerous studies have attempted to quantify erosion rates in historically mined areas, often driven by debates surrounding the most effective method for reclaiming land disturbed by recent (late twentieth century) surface mining activities (Soulliere and Toy, 1986; Toy and Hadley, 1987). Such research has indicated that erosion and sediment transfer rates are significantly higher in former mining landscapes than in comparable unmined areas (Lusby and Toy, 1976; Tarolli and Sofia, 2016). This situation is exacerbated even further in former metal mining areas, where the phytotoxic nature of heavily contaminated mine sediments reduces the capacity for vegetation cover resulting in highly unstable surface deposits (Ostrander and Clark, 1991). Previous studies of erosion at abandoned mines have, however, tended to focus on either the role of individual geomorphic processes (Haigh, 1980; Davies and White, 1981; Esling and Drake, 1988) or particular landform characteristics (Nyssen and Vermeersch, 2010; Martín-Moreno et al., 2013), meaning that our ability to fully understand the relative contribution of the wide range of interrelated factors influencing erosion rates is still limited.

This current study integrates repeat terrestrial laser scanning (TLS) and portable X-Ray Fluorescence (pXRF) survey to quantify contaminated sediment flux at Whitesike and Bentyfield mines, two adjacent abandoned lead mines located along Garrigill Burn, a tributary of the South Tyne in the North Pennine uplands, Cumbria, UK. The novel sediment budget approach, based on high resolution quantification of surface change and sediment contamination, demonstrates a rigorous methodology for investigating abandoned mines and provides valuable insights into the processes determining rates of contaminant flux in heavily disturbed landscapes. The study site represents an ideal case study for assessing the significance of contaminated sediment flux in former metal mining districts worldwide. Significant documented erosion and water quality issues sit awkwardly alongside the diverse and sometimes competing designation priorities of administrative bodies responsible for the preservation of the natural and cultural heritage environments. This range of challenges and pressures are characteristic of the complex multifaceted and interdisciplinary nature of abandoned mines, making the key findings from the study transferable to the management of other former mining landscapes worldwide.

2. Study site

Whitesike and Bentyfield mines are a pair of adjacent historical lead mines located ~5 km southeast of Alston, Cumbria, UK (54°46'36.48" N, 2°23'07.84 W) (Fig. 1). The mines occupy a small (3.51 km^2), steep catchment in the middle reaches of Garrigill Burn, an east-west flowing tributary of the upper South Tyne. Catchment elevations range from 330 m AOD at the confluence with the South Tyne to 614 m AOD at the watershed with the Nent catchment on Flinty Fell, with an overall channel gradient approaching 9%. The steep, narrow valley and mining remains located in close proximity to the stream channel provide minimal storage sites for colluvial deposits — a fairly typical situation within upland mining districts such as the North Pennines.

The underlying bedrock geology in the catchment consists of the Carboniferous cyclothems that are typical of this area of the Alston Block; primarily involving successive sequences of limestones, sandstones, siltstones, and mudstones. Extensive mineralisation of the numerous faults within these deposits occurred during the early Permian (ca. 290 Ma) and resulted in the rich mineral veins for which the North Pennine

Orefield is internationally renowned (Stone et al., 2010). Galena (lead ore) and sphalerite (zinc ore) are the most abundant sulphide minerals occurring throughout the orefield and have been the focus of much of the historical mining activity, with the galena typically also bearing relatively high levels of silver (Dunham, 1990; Dunham et al., 2001).

Garrigill Burn is included within the Water Framework Directive (WFD) water body covering the South Tyne from upstream of Garrigill to the confluence with Black Burn. Recent water quality monitoring on behalf of the Environment Agency has indicated that this section of the upper South Tyne is failing its Environmental Quality Standards (EQS) for zinc (Zn) and for cadmium (Cd), with Garrigill Burn known to be one of the primary sources of metal loading for the main river (Atkins Ltd, 2010b). Of the five mine sites within the upper South Tyne catchment that have been included within the Mine Waste Directive (MWD) inventory of abandoned mines known to be causing serious environmental impacts, three are located along Garrigill Burn (Whitesike Mine, Bentyfield Mine, and Brown Gill Mine) (Environment Agency, 2014).

Water sampling from locations along Garrigill Burn indicate that this tributary contributes up to 34.1% of the total Zn and 35.7% of the dissolved Zn loadings recorded at the Alston gauging station, the downstream WFD compliance point for the South Tyne (Atkins Ltd, 2010b). Percentage contributions from Garrigill Burn to cadmium loadings in the South Tyne at Alston are lower but still significant (up to 25%). Lead (Pb) does not exceed the EQS at the Alston gauge, but Garrigill Burn is again the primary source, contributing up to 30.9% of the total Pb and 34.3% of the dissolved Pb loadings for the upper South Tyne. Importantly, although the EQS for Pb was not exceeded at Alston, the combined contribution from the upper South Tyne and the Nent meant that it has been exceeded farther downstream at Featherstone (Atkins Ltd, 2010a). With 56% of the Pb loading at Featherstone gauging station coming from the South Tyne, the contribution from Garrigill Burn is again clearly of significance in terms of meeting overall EQS requirements in the wider Tyne basin.

One limitation of the previous sampling work along Garrigill Burn was that all field visits coincided with generally low to moderate flow events (0.7–7.8 m^3/s), meaning that they are only representative of a limited range of flow conditions within the catchment (Atkins Ltd, 2010b). Although point source metal concentrations sampled at the outflows from the Whitesike and Bentyfield adits were high, their flow rates

were low, suggesting that their contribution to overall Garrigill Burn contaminant levels is relatively small in comparison to other diffuse sources. Identifying the sources of these diffuse inputs, and in particular the sediment inputs likely to be of significance during high flow conditions, was a key focus for this current research.

The documented history of ore extraction at Whitesike and Bentyfield mines primarily covers the period from the late seventeenth century until their abandonment in the early 1900s, although archaeological surveys suggest that the length of active mining almost certainly extends back much further (Oakey et al., 2012; Railton and Wooler, 2012). Surface remains related to historical mining operations include mine adits, dressing floors (ore processing areas), a crushing mill wheel-pit, a two-storey mine shop, and multiple waste heaps associated with different stages of the extraction and processing workflow. Whitesike and Bentyfield mines are jointly under statutory archaeological protection as a nationally important Scheduled Monument (Historic England, 2015) and the majority of Whitesike Mine is also designated a Site of Special Scientific Interest (SSSI) because of the extensive calaminarian (metallophyte) grassland species found on the metal rich soils (Natural England, 2000). Despite these statutory designations, active erosion of the surface mining remains has been recognised as an ongoing problem for almost two decades (English Heritage, 2013). A programme of consolidation works to stabilise the mines was completed in 2012, informed by a geomorphological and flood risk assessment (Newson, 2012) and archaeological survey (Strickland and Wooler, 2012). Fieldwork for this current study commenced approximately five months after the stabilisation works had been completed and therefore at a time when the surface mining remains were considered to be at reduced risk of erosion.

3. Material and methods

3.1. Monitoring surface erosion - terrestrial laser scanning (TLS)

Repeat terrestrial laser scanning was used to monitor surface erosion at Whitesike and Bentyfield mines at approximately monthly intervals over an 18 month period (September 2012 to March 2014). Scanning was undertaken using a Riegl VZ-1000 time-of-flight based terrestrial laser scanner operating at a scan frequency of 300 kHz (RIEGL, 2013). Laser returns were collected every 0.03° within a 30-130° vertical and 0-360°

horizontal range, resulting in a potential maximum of 40,011,334 points per individual 5.5 minute scan. The scanner had a nominal maximum range of 450 m, but scan distances were typically much shorter than this because of the narrow width of the valley and local relief (mean distance from nearest scan station = 23 m).

Owing to the size (0.023 km^2) and variable topography of the survey area, scans were collected from 21 individual scan stations each month (Fig. 2). This was necessary in order to maintain approximately equal point spacing throughout the survey area (~20 mm) and avoid large areas of occlusion. These scans were broadly divided into three survey areas: Bentyfield Mine (13 scans; 14,013 m^2), Whitesike Mine (6 scans; 6444 m^2), and the western tailings heaps that originally served as waste dumps for both mines (2 scans; 2144 m^2). To aid the registration of the multiple point clouds, a network of additional reflective target markers (n = 20) was established throughout the survey area. The locations of the scan stations and target positions were recorded using a Leica 1200 differential GPS and marked with semipermanent survey stakes, allowing the accurate relocation of the survey tripod and reflective targets each month. Adverse weather conditions and equipment issues during five survey visits (December 2012, February/April/July 2013, February 2014) meant that only 14 out of 19 TLS data sets were fully captured.

Processing of the TLS data was undertaken in RiScan Pro v1.7.9 and involved the filtering of nonground points and the global georeferencing of the point clouds using the dGPS positions of the reflective targets. The coregistration of the multiple point clouds was then refined to a standard deviation error of <10 mm using the Multi Station Adjustment (MSA) tool, a cloud matching function based on an iterative closest point (ICP) algorithm. Registered monthly point clouds were exported as XYZ coordinates before being imported into ENVI v5.1 and interpolated to form 0.05 m resolution digital elevation models (DEMs).

3.2. Quantifying geomorphic change using DEM differencing

Geomorphic change occurring between successive TLS surveys was assessed using the DEM differencing method developed by Wheaton et al. (2010) and utilising the Geomorphic Change Detection (GCD) v6.1.8 add-in for ArcGIS v10.2. This change detection method includes consideration of spatial uncertainty in DEM error resulting from a number of user-defined input survey and terrain parameters, an approach that has been

successfully employed by a number of recent studies across a range of geomorphic contexts (Blasone et al., 2014; Kuo et al., 2015; Schaffrath et al., 2015).

Based on the premise that DEM error is spatially variable, the change detection method involved definition of a three input fuzzy inference system (FIS) including categories relating to point density, slope angle, and surface roughness — factors that have been demonstrated as useful indicators of elevation uncertainty (Milan et al., 2011; Schürch et al., 2011; Rychkov et al., 2012). Categorical thresholds (i.e., low, medium, high) for FIS input parameters were defined through consideration of local terrain and survey characteristics, as well as comparative examples from previous studies (Wheaton, 2008; Wheaton et al., 2010; Blasone et al., 2014).

The spatially variable error surfaces produced from sequential DEMs were combined to form a single propagated error raster, and a *t* score calculated the probability that elevation changes were real, based on the method outlined by Brasington et al. (2003). A 5 x 5 spatial coherence filter was subsequently applied to refine the DEM of Difference (DoD) uncertainty raster, based on the understanding that areas of erosion and deposition tend to occur in discrete units. A linear transform function was used to relate the output of this convolution filter to a cell-by-cell probability that the recorded elevation change was real, before these conditional probability values were combined with the FIS estimate of elevation uncertainty to generate a single updated probability surface. A probabilistic uncertainty threshold of 95% was used to either accept DoD cell values as real topographic change or reject them as relating to error (Wheaton et al., 2010).

Change detection analyses included pairwise comparison of each of the successive monthly TLS survey intervals and quantification of total changes occurring across the entire 18 month monitoring period (September 2012 – March 2014). Although the change detection method applied allows for the removal of spurious values caused by errors in the primary data, elevation change values within the resulting DoDs can still represent a combination of both real geomorphic change (e.g., erosion, deposition) and seasonal patterns of vegetation growth (Coveney and Fotheringham, 2011; Fan et al., 2014). To account for this issue, discrete morphological signatures visible in the DoDs were digitised as vector polygons within ArcGIS, based on the budget segregation method outlined by Wheaton *et al*. (2013). The TLS DEMs, aerial photographs and field observations were used to interpret the geomorphological process likely to have caused each mapped feature, with this information being added to the polygon data as tabular attributes. Elevation change values extracted

to each of these process categories were converted to mass using a bulk density of 1.674 ±0.18 t m^{-3}, based on an average of eight sediment samples taken from across the mined area.

3.3 X-Ray Fluorescence (XRF) survey

A field portable X-Ray Fluorescence (pXRF) survey was conducted on 15-17 August 2014 using a Niton XLT792 XRF analyser to characterise contaminant levels within surface soils around Whitesike and Bentyfield mines. Conditions over the three survey days were consistently dry, meaning surface moisture levels remained constant throughout. Zinc (Zn) and lead (Pb) were the main two metals historically extracted in the area and so analysis focused on understanding the spatial variation in their concentrations. Although cadmium (Cd) was identified as another metal of significance in terms of downstream water quality, large errors associated with the retrieval of this element during the field pXRF survey (mean error = 55%) meant that it was removed from subsequent analyses.

The pXRF unit was operated in bulk soil mode with the measurement analysis time set to 120 seconds, as recommended by Kilbride et al. (2006) and Shuttleworth et al. (2014). Surface debris was removed and the soil lightly compacted where necessary in order to present a flat surface to the sensor optics (Ridings et al., 2000). The accuracy of the internal calibration was checked at the beginning and end of each survey using analysis of appropriate certified reference material (CRM, till 4). The CRM concentrations measured in the field by the pXRF were all within ±14% of the reference value for Pb (σ = 4.9) and ±8% for Zn (σ = 6.4).

In situ pXRF measurements were recorded at 120 locations based on a predetermined stratified sampling strategy and positioned using a Garmin Etrex 10 handheld GPS (Fig. 2). This sampling approach categorised sample locations into relevant geomorphological landform units and whether they related to mine or non-mine (e.g., 'natural' colluvium) sediments (Table 1). The main focus of the survey was to characterise sediment contaminant variation across the mine sites themselves, and so 105 measurements were taken along a 900 m reach of Garrigill Burn covering the extent of Whitesike and Bentyfield mines. To better understand the broader sediment dispersal implications of the mine survey, an additional five measurements were taken from channel sediments located farther downstream along Garrigill Burn and ten measurements along the main River South Tyne, five upstream and five downstream of the confluence with Garrigill Burn (Fig. 1).

A random subsample of 20% (n = 24) of the pXRF measurement locations were selected for additional comparative laboratory analyses (Table 1). This sample size was deemed sufficient to include a range of readings within each of the different geomorphological sample units and so test the accuracy of the field measurements. Following the recording of the in situ pXRF measurement at these locations, a soil sample of the immediate area was collected using a plastic trowel to avoid potential contamination. Laboratory analyses of the subset of field samples were undertaken to provide comparative reference data against which to validate the field pXRF measurements. Soil samples were initially oven dried at 40°C then sieved at 2 mm before being ground and homogenised using an agate ball mill and passed through a 250 µm sieve (Ridings et al., 2000).

The same samples were then analysed using microwave-assisted acid extraction and inductively coupled plasma optical emission spectroscopy (ICP-OES). Subsamples weighing 150 mg were microwave digested in an acid solution of 4 ml H_20_2, 9 ml HNO_3, 3 ml HCL, and 2 ml HF (USEPA method 3052) before being filtered through Whatman glass microfibre filter papers. The filtrate was diluted to 50 ml using deionised water, and Pb and Zn concentrations were then determined using ICP-OES. The accuracy of the laboratory method was checked through analysis of samples of Certified Reference Material CRM BCS 362 (mine tailings) and CRM 7002 (light sandy soil). The relative percent difference (RPD) between the concentrations in each CRM and that measured by the ICP-OES was <5% for Pb and for Zn.

To further explore spatial variability in surface contaminant levels, the handheld GPS positions relating to the sample locations were linked to the tabular pXRF results and imported into ArcGIS v10.2. Contaminant values at unsampled locations were then estimated through interpolation (ordinary kriging) of the measured sample points, with separate modelled surfaces being produced for Pb and Zn. This approach has been shown to enhance the ability to identify spatial trends and contaminant hotspots from sample pXRF data (Carr et al., 2008; Hürkamp et al., 2009). Map algebra within ArcGIS was then used to combine the interpolated contaminant data with the surface change results from the TLS, providing estimates of contaminant mass flux for Pb and Zn. This involved the conversion of the volumetric change raster to mass using the average bulk density value, followed by the calculation of per-pixel contaminant flux through combination with the interpolated XRF results. The wider significance of the XRF results was assessed through comparison with available soil guideline values (SGVs) (Table 2).

4. Results

4.1. Rates and processes of surface change

Total net surface change across the full survey area during the 18 month period of TLS monitoring was overwhelmingly erosional, with the results indicating that the mined area contributed ~434 t (260 m^3) of sediment to Garrigill Burn, equivalent to 289 t a^{-1} (173 m^3 a^{-1}). The sediment budget constructed from the full TLS monitoring results (Fig. 3) displays the relative contribution of the different geomorphic drivers of change and highlights the dominance of certain erosional processes. Gullying accounted for ~60% (268 t) of all the recorded erosion from the overall survey area, with bank erosion contributing ~30% (134 t). Of the other erosion processes identified during the monitoring work, only diffuse slope erosion (21 t) and mass movements (13 t) recorded more than 10 t of mass loss. The other notable feature visible in the total sediment budget is the lack of sediment storage relative to the magnitude of recorded erosion (Fig. 3). A total of just 15.6 t of deposition was recorded across the entire mined area, representing only ~3% of the eroded material. These results indicate that the remaining ~97% of the eroded material was conveyed out of the immediate study area via Garrigill Burn and potentially therefore into the main River South Tyne system.

Spatial variation in the occurrence and magnitude of different erosion processes was clearly visible in the change detection results across the two mines (Figs. 4 and 5). Although overall net change at each area was erosional, the magnitude of erosion was far greater for the western tailings heaps (277 t) than for either Whitesike (104 t) or Bentyfield (53 t) mines. This was despite the tailings heap survey area being just 2144 m^2, compared with 6539 m^2 for Whitesike and 18,905 m^2 for Bentyfield. The substantial amount of erosion from the tailings heaps is primarily the result of the progressive development of a large gully system in the west-facing slope of the tip (Figs. 6 and 7). Four distinct gullies were identified, including one major central gully that accounted for ~262 t of eroded material — equivalent to 95% of all net erosion from the tailings heap and >60% of the total net erosion for the entire mined area. Recorded deposition on the tailings heaps was minimal (0.7 t) owing to the direct connection between the base of the slopes and the main channel of Garrigill Burn, which flows through a culvert immediately below the tips. Diffuse slope erosion was recorded across large sections of the mined area, resulting in relatively low magnitude (20.6 t) but spatially

extensive surface change. The unvegetated and exposed slopes of the tailings heaps were affected most by diffuse slope erosion (12.1 t), with Whitesike (3.9 t) and Bentyfield (4.6 t) mines recording comparably less surface change from these processes.

In contrast, surface changes recorded across Whitesike and Bentyfield mines were dominated more by processes associated with the main channel of Garrigill Burn than by slope processes (Figs. 4 and 5). Bank erosion resulted in 90 t of erosion at Whitesike Mine and 44 t at Bentyfield. This bank erosion involved individual large-scale collapses and slower progressive erosion from diffuse subaerial processes and direct entrainment of basal bank deposits. Particularly significant bank collapses were recorded adjacent to the lower dressing floor (37 t) and opposite the upper dressing floor (52 t) at Whitesike Mine and between the mine shop and dressing floors at Bentyfield Mine (37 t).

Mass movements (excluding bank failures) were another significant process at Bentyfield Mine in particular, resulting in ~13 t of erosion during the 18 month monitoring period (Figs. 4 and 5). The largest example of this was a substantial landslide on the north-facing slope of the main Bentyfield spoil heap, which monitoring revealed to be a relatively slow-moving rotational failure. Although the downslope displacement of the overall landslide was gradual, uplift of the toe during rotational movement periodically introduced moderate amounts of sediment into Garrigill Burn through shallow basal failures. The base of the landslide was directly adjacent to the stream channel with little capacity for long-term sediment storage, meaning that the mass movement provided a continuous but small-scale supply of mine waste sediments to Garrigill Burn and the wider stream network.

4.2. Temporal variability in process rates

The approximately monthly frequency of TLS monitoring enabled high resolution temporal variation in the pattern and magnitude of surface change to be quantified. These results indicate that the erosion of the mine deposits was highly episodic rather than overtly seasonal in character, with a prominent peak in rates of surface change between May and June 2013 (Fig. 8). For example, ~59 t of erosion occurred at Whitesike Mine during May 2013, equivalent to 57% of the entire net surface change for this mine area. This peak in erosion rate was experienced across the majority of the mined area and was dominated by extensive bank

erosion along Garrigill Burn and incision along concentrated flow paths, suggesting the occurrence of a high intensity rainfall event and associated high flow conditions. This peak likely relates to a storm event that occurred on 18 May, resulting in 27.44 mm of rainfall and the highest ever recorded peak flow of 335.2 $m^3 s^{-1}$ at the nearest gauging station on the main South Tyne at Alston, ~5.2 km away from Whitesike Mine (Fig. 8A). For context, this peak flow was 2.4 times the median annual maximum discharge for the South Tyne at Alston (*Qmed* = 139.2 $m^3 s^{-1}$); the recorded daily mean discharge of 59.5 $m^3 s^{-1}$ for the event is 1% of the time. Secondary peaks in surface change did occur at other times, such as the very large (~23 t) bank collapse opposite the Whitesike Mine lower dressing floor in September 2012 (Fig. 8C). However, these tended to be more isolated occurrences relating to specific local conditions or precursory patterns of change, such as the progressive undercutting of stream banks prior to large-scale collapse.

The detailed time series from the main gully system on the west-facing slope of the tailings heaps provides a useful example of the interactions between internal topographic adjustment and external environmental trigger factors (Figs. 7, 8B). The period recording the greatest amount of change was again the May-June 2013 survey interval, in which the majority of the gully experienced considerable morphological adjustment. This included significant incision along much of the gully floor, including a depth change exceeding 1.4 m in the upper gully area. Similarly, the prominent gully sidewall collapse between November 2012 and January 2013 potentially relates to external forcing in the form of large rainfall events in late November and December 2012. For example, the South Tyne station at Alston recorded 24.9 and 48.6 mm of rain on 25 and 26 November respectively,; followed by a further 20 mm on 8 December and 29.2 mm on 20 December (Fig. 8A). Other changes are likely to be the result of freeze-thaw and snowmelt, especially the extensive widening of the upper gully profile during January and May 2013.

Small-scale changes were, however, taking place throughout the year between the major weather-related erosional changes (Fig. 8). These low magnitude changes appear to be caused by a combination of small-scale sidewall collapses, downslope gravitational movement of eroded colluvial sediments, and animal activity (trampling, burrowing). For example, although the net change results indicate only moderate erosion between January and May 2013, the DoDs actually show that the gully underwent considerable internal modification owing to extensive cross-sectional and headward enlargement (Fig. 7). Interestingly, the majority of the eroded material was deposited on the central gully floor and remained there in temporary

storage until the major erosional event in May 2013, with the sediment export for this event therefore relating to further primary erosion of the gully and to the remobilisation of previously deposited sediments. These results suggest that temporal variation in the magnitude of surface change across the mined area was dominated by large-scale erosional events, but that low magnitude changes were occurring throughout the year; these have an important preparatory role in determining temporal fluctuations in sediment yields.

4.3. Mine-scale spatial variability in Pb and Zn concentrations

The results of the pXRF survey of the mine area show considerable variability in surface metal concentrations for Pb and Zn. Figure 9 shows the variability in metal concentrations between the different sample categories used in the initial field survey. Kruskal-Wallis H tests were conducted to determine if levels of Pb and Zn were significantly different between the three broad sample categories relating to mine, non-mine, and channel sediments. Although the results showed that there was no statistically significant difference in Pb between the three categories, $\chi^2(2) = 3.332$, $p = 0.1890$, there was a statistically significant difference in Zn concentrations, $\chi^2(2) = 8.551$, $p = 0.0139$. A post-hoc Mann-Whitney U (Wilcoxon rank-sum) test indicated that the only pair of categories to differ significantly in terms of Zn concentrations were the channel and mine sediments ($Z = -2.823$, $p = 0.0048$). The significance of these results is that, although landforms and deposits at the mine can be visually characterised in terms of their likely origin and formation, there is generally no equivalent distinction based solely on the levels of Pb and Zn in the corresponding sediments. This in turn implies a high degree of contaminant dispersal and mixing of sediments during the active mining period and through post-abandonment reworking.

The mean Pb concentration recorded in the field was 6480 mg kg^{-1}, with an overall range between a minimum of 60 and maximum of 78,000 mg kg^{-1} (Table 3). Analysis of the sample point values and interpolated surface (Figs. 10A, 11A) indicate clear spatial variability in Pb concentrations across the mined area, with notable hotspots in particular locations. The Pb levels are particularly elevated in the vicinity of the lower dressing floor of Whitesike Mine, with values here reaching the maximum recorded level of ~78,000 mg kg^{-1}. Another area of very high Pb concentrations (>30,000 mg kg^{-1}) was recorded farther upstream around the Bentyfield dressing floor and crushing mill, in this case extending across both banks of

Garrigill Burn. The third main area of high Pb concentrations was located on the unvegetated slopes of the tailings heaps to the west of Whitesike Mine (Fig. 10A). These values are markedly lower than those on the dressing floors but are still in the region of 10,000-15,000 mg kg^{-1}. Smaller hotspots with lower concentrations are found elsewhere across the mined area, including in the sediments immediately adjacent to the Whitesike Mine and Colonel's Level adits (~9000-12,000 mg kg^{-1}). Significantly, as well as hotspots of very high Pb concentrations, the results also indicate that 88% of all samples taken across the mined area were in excess of the UK residential / allotment soil guideline values and 84% were in excess of all available recommended guideline values for Pb (Table 2). All of the Pb values for the 20 channel sediment samples taken across the mined area were over 18 times greater than the threshold effects level (TEL) and 7 times greater than the probable effects level (PEL) guidelines specified by NOAA (Table 2).

The mean Zn concentration recorded across the mined area was 3060 mg kg^{-1}, with a range between 36 and 69,920 mg kg^{-1} (Table 3). The spatial distribution of Zn concentrations across the mined area shows marked similarities to those for Pb, with a notable concentration of very high levels around the Whitesike lower dressing floor, including the maximum recorded value of ~70,000 mg kg^{-1} (Figs. 10B, 11B). The Bentyfield dressing floor area also recorded high levels of Zn within the surface sediments (~5000-15,000 mg kg^{-1}), with smaller hotspots again identified in sediments adjacent to the main adit entrances (~2000-10,000 mg kg^{-1}). The Zn levels measured on the tailings heaps to the west were consistently high (>10,000 mg kg^{-1}), probably reflecting the fact that these waste heaps were never subsequently reprocessed to extract zinc, as occurred at other locations in the North Pennines (Dawson, 1947). Although there are no UK soil guideline values currently available for Zn, the results indicate that 65% of all pXRF sample measurements across the mined area were in excess of the recommended Dutch soil remediation intervention value and 96% were in excess of the equivalent target value (Table 2). All of the Zn values for the 20 channel sediment samples taken across the mined area were more than twice the specified TEL and 95% of these samples were also in excess of the specified PEL (Table 2).

4.4. Catchment-scale flux of contaminated sediments

The wider dispersal of contaminated sediments from the mined area was assessed through additional pXRF measurements taken from channel sediments located farther downstream along Garrigill Burn and from the main River South Tyne, up- and downstream of the confluence with Garrigill Burn (Fig. 1). Figure 11 clearly shows that stream sediment concentrations of Pb and Zn along Garrigill Burn increase with distance downstream. This trend continues beyond Whitesike and Bentyfield mines, with concentrations continuing to increase until the confluence with the South Tyne. The Pb concentrations increase from 1190 mg kg^{-1} for the sample point farthest upstream of the two mines to 4520 mg kg^{-1} at the confluence with the South Tyne. Similarly, Zn concentrations increase from 520 mg kg^{-1} at the upstream survey extent to 6450 mg kg^{-1} at the confluence with the South Tyne. In both these cases it must be stated that the upstream sample points are still actually downstream of other mining sites and so are unlikely to represent natural background geological levels.

Analysis of the pXRF measurements taken along the main River South Tyne shows that the levels of Pb and Zn upstream of the confluence with Garrigill Burn are markedly lower than those taken downstream (Fig. 12). The mean Pb concentration upstream of the confluence was 220 mg kg^{-1} while that for the downstream samples was 940 mg kg^{-1}. Although these mean concentrations are clearly influenced by outlier values, the median results show a similar pattern, with a concentration of 220 mg kg^{-1} upstream of the confluence and 696 mg kg^{-1} for the downstream samples. Samples taken immediately up- and downstream of the confluence saw a rise in Pb values from 260 to 2190 mg kg^{-1}. The Pb concentrations then dropped to 620 mg kg^{-1} by the next sample point ~175 m downstream, remaining <750 mg kg^{-1} for all other downstream measurements. The mean Zn concentration upstream of the confluence with Garrigill Burn was 160 mg kg^{-1}, increasing to 1970 mg kg^{-1} for the equivalent downstream samples. The Zn concentrations saw a similar sharp increase immediately downstream of the confluence itself, with a change from 185 to 3045 mg kg^{-1}. Unlike Pb, Zn values remained elevated for a greater distance downstream, decreasing to a value of 470 mg kg^{-1} ~450 m away from the confluence. Although based on a relatively small number of samples, these results correspond with earlier coarser resolution sampling of metal levels along the entire River South Tyne. For example, sampling by Macklin (1996) showed an overall trend of decreasing Pb and Zn concentrations with distance downstream, but with more abrupt periodic variations reflecting inputs from tributary confluences, including Garrigill Burn, and the influence of localised valley floor geometry.

4.5. Comparison of in situ XRF measurements to ICP-OES

In situ field pXRF measured concentrations for Pb and Zn were generally lower than the equivalent values obtained using ICP-OES (Table 3). This underestimation of contaminant values by field-based pXRF measurements is common and typically relates to a combination of factors, including moisture content, physical matrix effects, and inhomogeneity between surface and substrate sediments (Kalnicky and Singhvi, 2001; Kilbride et al., 2006; Peinado et al., 2010). Direct comparison between field results and laboratory-analysed reference samples is therefore crucial in order to obtain a more accurate estimate of the true level of sediment contamination.

The mean Pb value from the ICP-OES analyses was 8895 mg kg^{-1}, compared with 4775 mg kg^{-1} for the field pXRF results of the equivalent samples. The minimum (133 mg kg^{-1}) and maximum (75177 mg kg^{-1}) Pb values were also markedly higher for the ICP-OES results. The Zn concentrations show a similar pattern, with the mean Zn values of 4090 and 2340 mg kg^{-1} for ICP-OES and pXRF respectively. The minimum and maximum ICP-OES Zn values were 165 and 19,360 mg kg^{-1}, both significantly higher than the field pXRF equivalents. Moisture content for the samples used in the laboratory analyses ranged between 8.81 and 38.18%, with a mean value of 19.53% and standard deviation of 7.18%.

Linear regression between the field pXRF and ICP-OES values for Pb indicates a strong positive correlation with an R^2 of 0.95 (p = <0.0005). Hürkamp et al. (2009) found a similar relationship (R^2 = 0.94) based on a comparable dataset and used the straight line gradient of their regression equation to apply a correction factor to their original field pXRF results (x 1.51). The equivalent straight line gradient for the present study was higher (1.92) but still broadly comparable to the 1.51 recorded by Hürkamp et al. (2009). Applying the full regression equation increases the mean of the corrected field XRF values to 11,030 mg kg^{-1}, compared with only 5890 mg kg^{-1} for the raw field measurements (Table 3). The maximum Pb concentration for the corrected data set increases to 149,340 mg kg^{-1}.

The relationship between the field pXRF and ICP-OES values for Zn is less strong than for Pb but still shows a moderate-strong positive correlation (R^2 = 0.68, p = <0.0005) and a straight line gradient of 1.32. Applying the equation from a linear regression between these variables increases the mean of the corrected field XRF

values to 4924 mg kg^{-1}, compared with an original raw field value of 2968 mg kg^{-1}. The maximum Zn concentration increases from 69,920 mg kg^{-1} for the raw field pXRF data to 93,440 mg kg^{-1} for the corrected data (Table 3).

5. Discussion

5.1. Geomorphic drivers of erosion and contaminant release

Erosion of surface remains at Whitesike and Bentyfield mines is mobilising sediments with high concentrations of Pb and Zn and delivering them to the wider fluvial system. Integrating the results of the TLS and pXRF surveys allows total contaminated sediment flux from the mined area to be estimated and partitioned into the relative contributions from different geomorphic drivers. Together, these results suggest that there was a net export of ~4.59 t of Pb and 2.14 t of Zn during the 18 month monitoring period (Fig. 13). The tailings heaps were the primary source of eroding sediments across the mined area, mainly owing to the development of a large gully system on the west-facing slope. Gullying across the overall survey area released an estimated 3.09 t of Pb and 1.22 t of Zn, with the majority of this originating from the western tailings heaps. Erosion of abandoned mine deposits through rilling and gullying has been identified in a number of previous studies (Haigh, 1980; Hancock et al., 2008), with the lack of vegetation and steep slopes on waste heaps often making these landforms particularly susceptible (Gozzard et al., 2011).

The main concentrations of Pb and Zn were located across the lower dressing floor at Whitesike Mine, reflecting the nature of the processing activities that took place in this area (Fig. 10). Although monitoring revealed the upper surface of the dressing floor to be relatively stable, extensive lateral erosion of the banks of Garrigill Burn was recorded here. This is of particular concern given that the highest in situ pXRF levels for Pb (~78,000 mg kg^{-1}) and Zn (~70,000 mg kg^{-1}) from the entire mined area originated from bank samples in this location. A similar situation was found farther upstream at the Bentyfield dressing floor, where high levels of Pb (~35,000 mg kg^{-1}) and Zn (~15,000 mg kg^{-1}) have been recorded in areas experiencing moderate but persistent rates of bank erosion. Across the overall study area, bank erosion contributed 23% (1.07 t) of the total estimated Pb export and 32% (0.7 t) of the total Zn export (Fig. 13).

Although gullying of the tailings heaps and bank erosion along Garrigill Burn were the dominant geomorphic processes leading to the mobilisation of contaminated sediments, numerous other processes were also recorded (Fig. 4). Understanding the distribution and relative contribution of these lower magnitude processes is important as the pXRF results indicate that ~84% of all sediments sampled were in excess of available recommended soil guideline values for Pb and ~65% in excess of all available values for Zn. Similarly, the lack of clear separation between pXRF values for the different stratified sample categories (Fig. 9, section 4.3) indicates a high degree of mixing of sediments or leaching of contaminants between primary mine deposits and the local sedimentary environment. This demonstrates that erosion of any deposit within the vicinity of the mine is potentially mobilising highly contaminated and damaging sediments to the wider environment.

Even with high resolution TLS DEMs, however, actually identifying the relative contribution of specific low magnitude drivers of diffuse erosion can be difficult, unless the processes themselves can be directly observed in the field. For example, needle-ice formation and associated sediment detachment was clearly visible on a section of the dressing floor slope at Bentyfield Mine in December 2012 — a process that is known to influence variations in seasonal sediment yields in upland catchments (Prosser et al., 2000). However, it is likely that other unrecorded diffuse slope processes were also occurring, including wind erosion, sheetwash, and soil creep, all of which have also previously been documented at other abandoned mines (Esling and Drake, 1988; Toy, 1989; Merrington and Alloway, 1994).

Depositional processes were negligible in comparison with the overall magnitude of erosion, representing just ~3% of the total net erosion recorded. This can be explained by the proximity of the mine remains to the main stream channel and the corresponding lack of available storage areas on which eroded sediments could be deposited. For example, recorded deposition on the tailings heaps was only 0.7 t owing to the direct connection between the base of the tips and the main channel (Fig. 6). Because proximity to water was an important requirement for many aspects of historical metal mining operations, it is highly likely that this level of sediment connectivity is typical of many other metal mines in similar upland landscapes. This high degree of coupling between the eroding mine sediments and the stream channel has important implications for the mobilisation and dispersal of heavy metal contaminants to the wider environment, a point that will be considered in more detail in section 5.4.

5.2. Temporal variation in contaminated sediment flux

Although surface changes occurred throughout the monitoring period, the TLS surveys demonstrate that the erosion of abandoned mines in upland environments is highly episodic and driven primarily by high magnitude, low frequency storm events. The pronounced peak in erosion recorded in the May-June survey interval was the result of the storm that occurred on 18 May 2013 (Fig. 8). This storm led to a record peak discharge of 335.2 $m^3 s^{-1}$, a daily mean discharge of 59.5 $m^3 s^{-1}$, and the highest ever recorded river level at the South Tyne gauging station in Alston (2.85 m; typical range for 90% of time is 0.16–1.90 m) (Environment Agency, 2017). This event caused extensive erosion across the entire mined area, with especially large-scale changes occurring close to the main channel of Garrigill Burn and along preexisting concentrated flow paths. More broadly, the storm also resulted in widespread flood damage across northern England (Durham County Council, 2013). Although erosion resulting from this single storm event dominated the overall sediment flux, it is also clear from the time series data that the relationship between large precipitation events, discharge, and the magnitude of net erosion is complex, with some of the largest events recording only minimal net surface change (Fig. 8). This reflects the different characteristics of the individual precipitation events, antecedent conditions and variability in rates of surface erosion and sediment mobilisation.

For example, the intensity, duration, and spatial coverage of large precipitation events are crucial in determining the magnitude and extent of surface change. Precipitation associated with the 18 May event was actually relatively moderate (27. 4 mm), but the peak flow and river stage for the South Tyne at Alston reached record levels, suggesting that the storm was potentially high intensity and short duration. Antecedent conditions were also potentially important here, with 83.5 mm of rain falling during the 10 days leading up to the 18 May, meaning that catchments could have been near their moisture-holding capacity by the time the main storm occurred.

In comparison, the largest precipitation event during the monitoring occurred on 27 July 2013 (65.7 mm), but this date recorded only a moderate mean flow (16.7 $m^3 s^{-1}$) and no net erosion (Fig. 8). The reduced South Tyne discharge for this event is at least partially attributable to a period of relatively dry antecedent weather,

with only 28.5 mm of total rainfall during the preceding 21 days. Similarly, precipitation on 23 December 2013 was notably higher than the May 2013 event (39.4 mm); but the peak flow on the South Tyne was ~2.8 times less (119.9 $m^3 s^{-1}$), the maximum stage was over 90 cm lower, and recorded erosion was relatively low. In this case, the event followed a period of relatively prolonged rainfall, with 107.4 mm recorded over the preceding 10 days, indicating that other factors were of importance in determining levels of erosion along Garrigill Burn. For example, the gauging station at Alston is ~5 km away from Whitesike Mine. Therefore, a localised high intensity rainfall event in Alston may not have actually been significant farther upstream in the South Tyne catchment, and equally, high flow events recorded at the Alston gauging station could be reflecting localised storms from tributaries other than Garrigill Burn.

Sediment production and supply are also crucial in determining temporal variation in sediment flux and the observed disparities between precipitation events and net erosion rates. The time series from the main gully system on the western tailings heaps demonstrates this relationship very effectively (Fig. 7). The period from January to May 2013 saw extensive erosion of the upper gully but with the majority of the eroded material being retained in colluvial storage. The 18 May event then mobilised this stored sediment, resulting in a peak in net erosion for that month. In contrast, erosion in the months leading up to the 23 December event was relatively minor, meaning that even though this rainfall event was higher magnitude there was minimal sediment available and so the overall net surface change was limited. These data clearly suggest that, although large precipitation events are significant in driving the timing of surface processes, the specific intensity duration and spatial location of a storm, as well as the presence of readily available sediment, are crucial factors in determining the actual impacts that occur. The significance of high magnitude storms in driving the erosion of abandoned mines and release of contaminated sediments has been recognised in previous studies. Olyphant et al. (1991) found that low frequency, high magnitude rainfall events occurring in late spring are particularly effective at increasing sediment yields from abandoned mines, due to a combination of direct erosion and the flushing of previously eroded colluvial sediments from the slopes. The results from Whitesike and Bentyfield clearly fit this pattern but it should be noted that high intensity storms occurring at any time of year can result in a dramatic increase in erosion rates at abandoned mines (Evans et al., 2000). High intensity storms such as these can dominate patterns of annual erosion and contaminant flux, with Smith and Olyphant (1994) recording over 50% of the annual sediment yield from an abandoned coal

mine in the midwestern USA as being produced by only 15% of the annual storms. Numerous other studies have also highlighted the dominance of diffuse sediment-borne contaminant inputs over point source metal contributions during high flow events, even if the actual sediment sources have not been specifically quantified (Mayes et al., 2008; Byrne et al., 2013). With the frequency and intensity of extreme precipitation events predicted to increase under projected climate scenarios (Kirtman et al., 2013), it appears highly likely that the large-scale erosion of heavily contaminated mine deposits will also increase in future decades (Macklin et al., 2006; Foulds et al., 2014).

5.3. Fluvial dispersal of contaminated sediments

The lack of sediment storage within the mined reaches of Garrigill Burn means that highly contaminated eroded mine sediments are often directly coupled with the main stream and the wider Tyne catchment. The high sediment delivery from Garrigill Burn reflects the steep, narrow valley and close proximity of the mining remains to the stream channel — a common situation in many upland mining areas where operations were reliant on water resources and water power. In such settings, erosion of mining remains is active and coupling between hillslopes and channels is high as floodplains are small and fragmented. Eroded contaminated sediments are therefore rapidly conveyed out of tributary systems such as Garrigill Burn before being attenuated through dispersal and storage within the wider Tyne catchment.

The pXRF results indicate that Pb and Zn levels in stream sediments increase with distance downstream along Garrigill Burn, with values rising well above all recommended guideline values (Fig. 11). This increase in metal levels is likely to relate to cumulatively increasing inputs from the mine deposits at Whitesike and Bentyfield, as well as contributions from additional downstream mining remains (e.g., at Beldy, Fig. 1). Measurements taken along the main South Tyne show the impact of sediment contributions from Garrigill Burn, with Pb and Zn levels increasing and remaining elevated for at least 400 m downstream (Fig. 12). The results demonstrate that sediment inputs to Garrigill Burn are clearly impacting the wider Tyne catchment, with most of the contaminated sediments originating from Whitesike and Bentyfield mines during infrequent but high magnitude storm events. This dispersal of contaminated mine sediments has

important implications for downstream water quality targets and our understanding of the broader catchment-scale patterns of heavy metal transfer (Miller, 1997; Dennis et al., 2009; Mayes et al., 2013).

5.4. Wider implications for the monitoring and management of abandoned mines

This study has demonstrated that correlating the scale and timing of sediment inputs with measured contaminant levels provides valuable insights into where and when episodic diffuse metal inputs are occurring. Such information is crucial when planning appropriate management or remediation schemes to reduce contaminated sediment inputs from abandoned mines. At Whitesike and Bentyfield, for example, the diffuse sediment contaminant load could be significantly reduced by targeting any future management work on just the west-facing slope of the tailings heaps, with contributions from other locations being relatively small in comparison. Any such management intervention would need to consider the nature of the process driving the mobilisation of the contaminated sediments (i.e., gullying) and be able to stabilise the slopes even during high magnitude storms when erosion and contaminant flux are typically at their highest.

From a methodological perspective, the combined use of TLS monitoring and pXRF sampling has proved effective at directly quantifying diffuse sediment inputs to river systems impacted by historical metal mining. With its ability to identify specific contaminated sediment source locations, this integrated methodology provides an important comparative approach to other studies that quantify diffuse inputs using water sampling and indirect mass balance estimates (e.g., Mighanetara et al., 2009). However, comparison of the in situ pXRF and laboratory ICP-OES analyses suggests that the field results could be underestimating actual metal levels by a factor of ~1.9 for Pb and ~1.3 for Zn (section 4.5), likely owing to a combination of moisture content and particle size (Binstock et al., 2009). The implication of this is that actual contaminant levels are likely to be appreciably higher and the wider environmental impacts more pronounced, with the results presented essentially therefore recording a best case scenario for current levels of contaminated sediment flux to Garrigill Burn.

Global estimates suggest ~349 million t of Pb and 713 million t of Zn were extracted worldwide up to the late twentieth century (Singer, 1995), with a considerable proportion being through relatively early, unregulated and uncontrolled operations (Nriagu, 1996; Price et al., 2011). Combined with recent

assessments indicating that there are at least 4900 noncoal abandoned mine sites throughout just England and Wales alone (Mayes et al., 2009), the scale of the global legacy from historical mining is considerable. Many of these abandoned mines are likely to share similar intrinsic (e.g., phytotoxic sediments, angle of repose waste heaps) and extrinsic (e.g., harsh or variable climates) factors that make them particularly susceptible to erosion. Because ~90% of metal contaminants in mined catchments are associated with sedimentary forms (Hudson-Edwards et al., 2008), it is therefore imperative that further research is directed toward developing our understanding of the drivers, rates, and timing of erosion on abandoned metal mines.

6. Conclusions

This study has quantified the role of eroding abandoned metal mines as ongoing source contributors of heavily contaminated sediments to fluvial systems. The erosion of abandoned mines is a significant and persistent issue, with 289 t a^{-1} of sediment entering Garrigill Burn from just two relatively small historical metal mines, equivalent to an estimated heavy metal contribution of ~3.06 t a^{-1} of Pb and 1.43 t a^{-1} of Zn. This ongoing release of Pb is equivalent to ~3% of the annual total production output from the two mines during their peak period of operation (1845-1900). Given the lack of storage capacity downstream of the mines along Garrigill Burn, we can assume that a high proportion of the eroded sediment is likely to reach the River South Tyne. In the absence of further stabilisation works, this process is likely to continue, with these two historical metal mines therefore acting as a significant source of Pb and Zn pollution for at least the foreseeable future.

Coupling between eroding mine sediments and stream channels is high, with only ~3% of the eroded material being deposited as colluvial material. This reflects a combination of factors, including the steep and narrow form of the valley, the proximity of the mine remains to the stream and direct connectivity between eroding landforms and the channel network. Gullying of poorly consolidated and unvegetated waste heaps was the dominant driver of erosion at the mines, accounting for ~60% of all recorded erosion from the entire survey area. Bank erosion accounted for a further ~30% of the total erosion, with the remaining ~10% attributable to a range of lower magnitude diffuse erosion processes and discrete but slow-moving slope failures.

Erosion at the mine sites, and therefore the corresponding release of contaminated sediments, is highly episodic rather than overtly seasonal in character, being driven by high magnitude, low frequency storm events. The surface sediments themselves display considerable spatial variation in their concentrations of heavy metals, relating primarily to the distribution of the different mining processes which took place across the site. Particularly high concentrations (up to ~78,000 mg kg^{-1}) were identified across the ore processing floors and in the tailings heap deposits to the west of the mined area; both areas also experienced considerable erosion in the form of bank collapses and gullying respectively. Importantly, however, the pXRF results also indicate that ~84% of all sediments sampled were in excess of all available soil guideline values for Pb and ~65% in excess of all available guideline values for Zn, indicating that any erosion across the majority of the mined area is potentially mobilising damaging levels of heavy metals.

Abandoned metal mines present a unique and complex set of interdisciplinary challenges to the global science and management communities. There is a need to carefully balance their potentially damaging legacy effects — particularly in the form of high erosion rates, phytotoxic surface sediments, and water quality impacts — against their role as ecological habitats for rare metallophyte plant communities (Batty, 2005) and as important cultural heritage archives (Howard et al., 2015; Kincey et al., 2017). This current study has provided valuable insights into the distribution and timing of contaminated sediment flux from abandoned mines, enhancing our understanding of such sites as heavy metal source locations and therefore bridging the gap to existing studies focused on the wider catchment implications of historical mining (e.g., Miller, 1997; Macklin et al., 2006; Foulds et al., 2014; Clement et al., 2017; Pavlowsky et al., 2017). Future research should focus on monitoring sediment source contributions from abandoned mines in a range of other physical and environmental contexts, with the overall aim being to enhance our understanding to a point where realistic predictions can be made about likely morphological responses and contaminant inputs under a variety of future management and climate scenarios.

Acknowledgements

This study was undertaken with the support of a PhD studentship provided by the Department of Geography, Durham University. The authors gratefully acknowledge the support of those involved in the fieldwork at

Whitesike and Bentyfield, as well as the laboratory staff in the Department of Geography at Durham University, especially Martin West, Amanda Hayton, Chris Longley, and Frank Davies. We thank Pippa Whitehouse and the five anonymous reviewers for providing constructive comments and feedback which helped to improve the manuscript.

References

Atkins Ltd, 2010a. North Pennines Metal Mines Monitoring Report. Catchment Monitoring - Nent, Atkins Limited, unpublished report for the Environment Agency.

Atkins Ltd, 2010b. North Pennines Metal Mines Monitoring Report. Catchment Monitoring - South Tyne, Atkins Limited, unpublished report for the Environment Agency.

Banks, V.J., Palumbo-Roe, B., 2010. Synoptic monitoring as an approach to discriminating between point and diffuse source contributions to zinc loads in mining impacted catchments. Journal of Environmental Monitoring, 12(9), 1684-1698.

Batty, L., 2005. The potential importance of mine sites for biodiversity. Mine Water and the Environment, 24, 101-103.

Binstock, D.A., Gutknecht, W.F., McWilliams, A.C., 2009. Lead in Soil - An examination of paired XRF analysis performed in the field and laboratory ICP-AES results. International Journal of Soil, Sediment and Water, 2(2), 1-6.

Blasone, G., Cavalli, M., Marchi, L., Cazorzi, F., 2014. Monitoring sediment source areas in a debris-flow catchment using terrestrial laser scanning. CATENA, 123, 23-36.

Brasington, J., Langham, J., Rumsby, B., 2003. Methodological sensitivity of morphometric estimates of coarse fluvial sediment transport. Geomorphology, 53(3–4), 299-316.

Brewer, P., Dennis, I.A., Macklin, M., 2003. The use of geomorphological mapping and modelling for identifying land affected by metal contamination on river floodplains, Department for Environment, Food and Rural Affairs (DEFRA).

Buchman, M.F., 2008. NOAA Screening Quick Reference Tables, Office of Response and Restoration Division, National Oceanic and Atmospheric Administration.

Byrne, P., Reid, I., Wood, P.J., 2013. Stormflow hydrochemistry of a river draining an abandoned metal mine: the Afon Twymyn, central Wales. Environ Monit Assess, 185(3), 2817-2832.

Carr, R., Zhang, C., Moles, N., Harder, M., 2008. Identification and mapping of heavy metal pollution in soils of a sports ground in Galway City, Ireland, using a portable XRF analyser and GIS. Environ Geochem Health, 30(1), 45-52.

Clement, A.J.H., Nováková, T., Hudson-Edwards, K.A., Fuller, I.C., Macklin, M.G., Fox, E.G., Zapico, I., 2017. The environmental and geomorphological impacts of historical gold mining in the Ohinemuri and Waihou river catchments, Coromandel, New Zealand. Geomorphology, 295, 159-175.

Coveney, S., Fotheringham, S., 2011. Terrestrial laser scan error in the presence of dense ground vegetation. The Photogrammetric Record, 26(135), 307-324.

Davies, B.E., White, H.M., 1981. Environmental pollution by wind blown lead mine waste: A case study in wales, U.K. Science of The Total Environment, 20(1), 57-74.

Dawson, E.W.O., 1947. War-time treatment of the lead-zinc dumps situated at Nenthead, Cumberland. Transactions of the Institution of Mining and Metallurgy, 56, 587-605.

Dennis, I.A., Macklin, M.G., Coulthard, T.J., Brewer, P.A., 2003. The impact of the October–November 2000 floods on contaminant metal dispersal in the River Swale catchment, North Yorkshire, UK. Hydrological Processes, 17(8), 1641-1657.

Dennis, I.A., Coulthard, T.J., Brewer, P., Macklin, M.G., 2009. The role of floodplains in attenuating contaminated sediment fluxes in formerly mined drainage basins. Earth Surface Processes and Landforms, 34(3), 453-466.

Dunham, K.C., 1990. Geology of the Northern Pennines Orefield, Volume 1 Tyne to Stainmore (2nd Edition). Economic Memoir of the British Geological Survey. British Geological Survey.

Dunham, K.C., Young, B., Johnson, G.A.L., Colman, T.C., Fossett, R., 2001. Rich silver-bearing lead ores in the Northern Pennines? Proceedings of the Yorkshire Geological and Polytechnic Society, 53(3), 207-212.

Durham County Council, 2013. Flooding Update: report of corporate management team, Durham County Council.

English Heritage, 2013. Heritage at Risk Register 2013: North West, English Heritage.

Environment Agency, 2007. The Unseen Threat to Water Quality: Diffuse Pollution in England and Wales Report - May 2007, Environment Agency, Bristol.

Environment Agency, 2014. Inventory of closed mining waste facilities, Environment Agency, Bristol.

Environment Agency, 2017. River and sea levels - River South Tyne at Alston.

Esling, S.P., Drake, L., 1988. Erosion of strip-mine spoil in Iowa and its implications for erosion models. Geomorphology, 1(4), 279-296.

European Commission, 2000. Directive 2000/60/EC of the European Parliament and of the Council of 23 October 2000 establishing a framework for Community action in the field of water policy

European Commission, 2006. Directive 2006/21/EC of the European Parliament and of the Council on the management of waste from the extractive industries.

Evans, K.G., Saynor, M.J., Willgoose, G.R., Riley, S.J., 2000. Post-mining landform evolution modelling: 1. Derivation of sediment transport model and rainfall–runoff model parameters. Earth Surface Processes and Landforms, 25(7), 743-763.

Fan, L., Powrie, W., Smethurst, J., Atkinson, P.M., Einstein, H., 2014. The effect of short ground vegetation on terrestrial laser scans at a local scale. ISPRS Journal of Photogrammetry and Remote Sensing, 95, 42-52.

Forth, R.A., 1999. The stability and contamination of some tips and tailings dams in Northern England. In: IMWA (Ed.), Mine water and environment for the 21st Century: conference proceedings. International Mine Water Association, Sevilla, Spain.

Foulds, S.A., Brewer, P.A., Macklin, M.G., Haresign, W., Betson, R.E., Rassner, S.M.E., 2014. Flood-related contamination in catchments affected by historical metal mining: An unexpected and emerging hazard of climate change. Science of The Total Environment, 476–477(0), 165-180.

Gozzard, E., Mayes, W.M., Potter, H.A.B., Jarvis, A.P., 2011. Seasonal and spatial variation of diffuse (non-point) source zinc pollution in a historically metal mined river catchment, UK. Environmental Pollution, 159(10), 3113-3122.

Haigh, M.J., 1980. Slope retreat and gullying on revegetated surface mine dumps, Waun Hoscyn, Gwent. Earth Surface Processes, 5(1), 77-79.

Hancock, G.R., Lowry, J.B.C., Moliere, D.R., Evans, K.G., 2008. An evaluation of an enhanced soil erosion and landscape evolution model: a case study assessment of the former Nabarlek uranium mine, Northern Territory, Australia. Earth Surface Processes and Landforms, 33(13), 2045-2063.

Historic England, 2015. Scheduled Monument List Entry: Whitesike and Bentyfield lead mines and ore works (1015832).

Howard, A.J., Kincey, M., Carey, C., 2015. Preserving the Legacy of Historic Metal-Mining Industries in Light of the Water Framework Directive and Future Environmental Change in Mainland Britain: Challenges for the Heritage Community. The Historic Environment: Policy & Practice, 6(1), 3-15.

Hudson-Edwards, K., Macklin, M., Brewer, P.A., Dennis, I.A., 2008. Assessment of metal mining-contaminated river sediments in England and Wales.

Hürkamp, K., Raab, T., Völkel, J., 2009. Two and three-dimensional quantification of lead contamination in alluvial soils of a historic mining area using field portable X-ray fluorescence (FPXRF) analysis. Geomorphology, 110(1–2), 28-36.

ITRC (Interstate Technology & Regulatory Council), 2008. Mine Waste Issues in the United States: A White Paper, Interstate Technology & Regulatory Council, Mining Waste Team, Washington, D.C.

Kalnicky, D.J., Singhvi, R., 2001. Field portable XRF analysis of environmental samples. Journal of Hazardous Materials, 83(1), 93-122.

Kilbride, C., Poole, J., Hutchings, T.R., 2006. A comparison of Cu, Pb, As, Cd, Zn, Fe, Ni and Mn determined by acid extraction/ICP–OES and ex situ field portable X-ray fluorescence analyses. Environmental Pollution, 143(1), 16-23.

Kincey, M., Gerrard, C., Warburton, J., 2017. Quantifying erosion of 'at risk' archaeological sites using repeat terrestrial laser scanning. Journal of Archaeological Science: Reports, 12, 405-424.

Kirtman, B., Power, S.B., Adedoyin, J.A., Boer, G.J., Bojariu, R., Camilloni, I., Doblas-Reyes, F.J., Fiore, A.M., Kimoto, M., Meehl, G.A., Prather, M., Sarr, A., Schaer, C., Sutton, R., van Oldenborgh, G.J.,

Vecchi, G., Wang, H.J., 2013. Near-term Climate Change: Projections and Predictability. In: T.F. Stocker, D. Qin, G.-K. Plattner, M. Tignor, S.K. Allen, J. Boschung, A. Nauels, Y. Xia, V. Bex, P.M. Midgley (Eds.), Climate Change 2013: The Physical Science Basis. Contribution of Working Group I to the Fifth Assessment Report of the Intergovernmental Panel on Climate Change. Cambridge University Press, Cambridge, United Kingdom and New York, USA.

Knighton, A.D., 1989. River adjustment to changes in sediment load: The effects of tin mining on the Ringarooma River, Tasmania, 1875–1984. Earth Surface Processes and Landforms, 14(4), 333-359.

Kossoff, D., Dubbin, W.E., Alfredsson, M., Edwards, S.J., Macklin, M.G., Hudson-Edwards, K.A., 2014. Mine tailings dams: Characteristics, failure, environmental impacts, and remediation. Applied Geochemistry, 51, 229-245.

Kuo, C.-W., Brierley, G., Chang, Y.-H., 2015. Monitoring channel responses to flood events of low to moderate magnitudes in a bedrock-dominated river using morphological budgeting by terrestrial laser scanning. Geomorphology, 235, 1-14.

Lewin, J., Davies, B.E., Wolfenden, P.J., 1977. Interactions Between Channel Change and Historic Mining Sediments. In: K.J. Gregory (Ed.), River Channel Changes. John Wiley & Sons, Chichester.

Luís, A.T., Teixeira, P., Almeida, S.F.P., Matos, J.X., da Silva, E.F., 2011. Environmental impact of mining activities in the Lousal area (Portugal): Chemical and diatom characterization of metal-contaminated stream sediments and surface water of Corona stream. Science of The Total Environment, 409(20), 4312-4325.

Lusby, G.C., Toy, T.J., 1976. An evaluation of surface-mine spoils area restoration in Wyoming using rainfall simulation. Earth Surface Processes, 1(4), 375-386.

Macklin, M.G., 1996. Fluxes and storage of sediment-associated heavy metals in floodplain systems: assessment and river basin management issues at a time of rapid environmental change. In: M.G. Anderson, D.E. Walling, P.D. Bates (Eds.), Floodplain processes. John Wiley and Sons, Ltd., pp. 441-459.

Macklin, M.G., Brewer, P.A., Balteanu, D., Coulthard, T.J., Driga, B., Howard, A.J., Zaharia, S., 2003. The long term fate and environmental significance of contaminant metals released by the January and March 2000 mining tailings dam failures in Maramureş County, upper Tisa Basin, Romania. Applied Geochemistry, 18(2), 241-257.

Macklin, M.G., Brewer, P.A., Hudson-Edwards, K.A., Bird, G., Coulthard, T.J., Dennis, I.A., Lechler, P.J., Miller, J.R., Turner, J.N., 2006. A geomorphological approach to the management of rivers contaminated by metal mining. Geomorphology, 79(3-4), 423-447.

Martín-Moreno, C., Martín Duque, J.F., Nicolau Ibarra, J.M., Hernando Rodríguez, N., Sanz Santos, M.Á., Sánchez Castillo, L., 2013. Effects of topography and surface soil cover on erosion for mining reclamation: the experimental spoil heap at El Machorro mine (Central Spain). Land Degradation & Development, n/a-n/a.

Mayes, W.M., Gozzard, E., Potter, H.A.B., Jarvis, A.P., 2008. Quantifying the importance of diffuse minewater pollution in a historically heavily coal mined catchment. Environmental Pollution, 151(1), 165-175.

Mayes, W.M., Johnston, D., Potter, H.A.B., Jarvis, A.P., 2009. A national strategy for identification, prioritisation and management of pollution from abandoned non-coal mine sites in England and Wales. I.: Methodology development and initial results. Science of The Total Environment, 407(21), 5435-5447.

Mayes, W.M., Potter, H.A.B., Jarvis, A.P., 2010. Inventory of aquatic contaminant flux arising from historical metal mining in England and Wales. Science of The Total Environment, 408(17), 3576-3583.

Mayes, W.M., Potter, H.A.B., Jarvis, A.P., 2013. Riverine Flux of Metals from Historically Mined Orefields in England and Wales. Water, Air, & Soil Pollution, 224(2), 1425.

Mayes, W.M., Anton, A.D., Thomas, C., Potter, H.A.B., Rudall, S., Amezaga, J.M., Gandy, C.J., Jarvis, A.P., 2015. National assessment of sediment-related diffuse mining pollution in England and Wales. Conference paper., ICARD & IMWA Annual Conference, Santiago, Chile.

Merrington, G., Alloway, B.J., 1994. The transfer and fate of Cd, Cu, Pb and Zn from two historic metalliferous mine sites in the U.K. Applied Geochemistry, 9(6), 677-687.

Mighanetara, K., Braungardt, C.B., Rieuwerts, J.S., Azizi, F., 2009. Contaminant fluxes from point and diffuse sources from abandoned mines in the River Tamar catchment, UK. Journal of Geochemical Exploration, 100(2–3), 116-124.

Milan, D.J., Heritage, G.L., Large, A.R.G., Fuller, I.C., 2011. Filtering spatial error from DEMs: Implications for morphological change estimation. Geomorphology, 125(1), 160-171.

Miller, J.R., 1997. The role of fluvial geomorphic processes in the dispersal of heavy metals from mine sites. Journal of Geochemical Exploration, 58(2), 101-118.

Natural England, 2000. Citation for Whitesike Mine and Flinty Fell SSSI, Natural England.

Newson, M., 2012. Geomorphological and flood risk management implications of the proposed Whitesykes and Bentyfield Mine restoration, Garrigill Burn, South Tyne.

Nriagu, J.O., 1996. A history of global metal pollution. Science, 272(5259), 223.

Nyssen, J., Vermeersch, D., 2010. Slope aspect affects geomorphic dynamics of coal mining spoil heaps in Belgium. Geomorphology, 123(1–2), 109-121.

Oakey, M., Radford, S., Knight, D., 2012. Alston Moor, North Pennines: Aerial investigation and mapping report, English Heritage.

Olyphant, G.A., Carlson, C.P., Harper, D., 1991. Seasonal and Storm-Related Aspects of Sediment Yield From a Rapidly Eroding Coal Refuse Deposit in Southwestern Indiana. Water Resources Research, 27(11), 2825-2833.

Ostrander, R., Clark, S., 1991. Soil heavy metal concentrations and erosion damage in upland grasslands in the Pennines, England. Water Air Soil Pollut, 59(1-2), 81-94.

Palumbo-Roe, B., Wragg, J., Banks, V.J., 2012. Lead mobilisation in the hyporheic zone and river bank sediments of a contaminated stream: contribution to diffuse pollution. J Soils Sediments, 12(10), 1633-1640.

Pavlowsky, R.T., Lecce, S.A., Owen, M.R., Martin, D.J., 2017. Legacy sediment, lead, and zinc storage in channel and floodplain deposits of the Big River, Old Lead Belt Mining District, Missouri, USA. Geomorphology, 299, 54-75.

Peinado, F.M., Ruano, S.M., González, M.G.B., Molina, C.E., 2010. A rapid field procedure for screening trace elements in polluted soil using portable X-ray fluorescence (PXRF). Geoderma, 159(1–2), 76-82.

Price, S.J., Ford, J.R., Cooper, A.H., Neal, C., 2011. Humans as major geological and geomorphological agents in the Anthropocene: the significance of artificial ground in Great Britain. Philosophical Transactions of the Royal Society A: Mathematical, Physical and Engineering Sciences, 369(1938), 1056-1084.

Prosser, I.P., Hughes, A.O., Rutherfurd, I.D., 2000. Bank erosion of an incised upland channel by subaerial processes: Tasmania, Australia. Earth Surface Processes and Landforms, 25(10), 1085-1101.

Railton, M., Wooler, F., 2012. Miner-Farmer Landscapes of the North Pennines AONB: Block 2A Landscape Survey, Wardell Armstrong Archaeology Ltd.

Ridings, M., Shorter, A.J., Smith, J.B., 2000. Strategies for the investigation of contaminated sites using field portable x-ray fluorescence (FPXRF) techniques. Communications in Soil Science and Plant Analysis, 31(11-14), 1785-1790.

RIEGL, 2013. RIEGL VZ-1000 Data Sheet.

Rychkov, I., Brasington, J., Vericat, D., 2012. Computational and methodological aspects of terrestrial surface analysis based on point clouds. Computers & Geosciences, 42, 64-70.

Schaffrath, K.R., Belmont, P., Wheaton, J.M., 2015. Landscape-scale geomorphic change detection: Quantifying spatially variable uncertainty and circumventing legacy data issues. Geomorphology, 250, 334-348.

Schürch, P., Densmore, A.L., Rosser, N.J., Lim, M., McArdell, B.W., 2011. Detection of surface change in complex topography using terrestrial laser scanning: application to the Illgraben debris-flow channel. Earth Surface Processes and Landforms, 36(14), 1847-1859.

Shuttleworth, E.L., Evans, M.G., Hutchinson, S.M., Rothwell, J.J., 2014. Assessment of Lead Contamination in Peatlands Using Field Portable XRF. Water, Air, & Soil Pollution, 225(2), 1-13.

Singer, D., 1995. World class base and precious metal deposits; a quantitative analysis. Economic Geology, 90(1), 88-104.

Singer, M.B., Aalto, R., James, L.A., Kilham, N.E., Higson, J.L., Ghoshal, S., 2013. Enduring legacy of a toxic fan via episodic redistribution of California gold mining debris. Proceedings of the National Academy of Sciences, 110(46), 18436-18441.

Smith, L.C., Olyphant, G.A., 1994. Within-storm variations in runoff and sediment export from a rapidly eroding coal-refuse deposit. Earth Surface Processes and Landforms, 19(4), 369-375.

Soulliere, E.J., Toy, T.J., 1986. Rilling of hillslopes reclaimed before 1977 surface mining law, Dave Johnston Mine, Wyoming. Earth Surface Processes and Landforms, 11(3), 293-305.

Stone, P., Milward, D., Young, B., Merritt, J., Clarke, S., McCormac, M., Lawrence, D., 2010. British Regional Geology: Northern England (Fifth Edition). British Geological Survey, Keyworth, Nottingham.

Strickland, J., Wooler, F., 2012. Whitesike and Bentyfield Mining Complex, Alston Moor, Cumbria. Desk-based Assessment, Archaeological Survey and Watching Brief., NP Archaeology Ltd.

Tarolli, P., Sofia, G., 2016. Human topographic signatures and derived geomorphic processes across landscapes. Geomorphology, 255, 140-161.

Toy, T.J., Hadley, R.F., 1987. Geomorphology and reclamation of disturbed lands. Academic Press, Orlando.

Toy, T.J., 1989. An assessment of surface-mine reclamation based upon sheetwash erosion rates at the Glenrock coal company, Glenrock, Wyoming. Earth Surface Processes and Landforms, 14(4), 289-302.

Turner, A.J.M., Braungardt, C., Potter, H., 2011. Risk-based prioritisation of closed mine waste facilities using GIS. In: R.T. Ruede, A. Freund, C. Wolkersdorfer (Eds.), International Mine Water Association Congress 2011 - Managing the Challenges, Aachen, Germany.

Wheaton, J.M., 2008. Uncertainty in Morphological Sediment Budgeting of Rivers. Unpublished PhD Thesis, University of Southampton, Southampton, 412 pp.

Wheaton, J.M., Brasington, J., Darby, S.E., Sear, D.A., 2010. Accounting for uncertainty in DEMs from repeat topographic surveys: improved sediment budgets. Earth Surface Processes and Landforms, 35(2), 136-156.

Wheaton, J.M., Brasington, J., Darby, S.E., Kasprak, A., Sear, D., Vericat, D., 2013. Morphodynamic signatures of braiding mechanisms as expressed through change in sediment storage in a gravel-bed river. Journal of Geophysical Research: Earth Surface, 118(2), 759-779.

Wray, D.S., 1998. The impact of unconfined mine tailings and anthropogenic pollution on a semi-arid environment – an initial study of the Rodalquilar mining district, south east Spain. Environ Geochem Health, 20(1), 29-38.

Table 1

Stratified sampling strategy for pXRF field survey and laboratory reference analyses

Category	Example context	No. of pXRF measurements	Paired laboratory analyses (20%)
Hillslope – non-mine	'Natural' undisturbed hillslope	15	3
Hillslope – mine	Spoil and tailing heaps	15	3
Floodplain – non-mine	Floodplain with no distinct mining features	15	3
Floodplain – mine	Dressing floors	15	3
Stream bank – non-mine	Bank comprised of non-mine sediments	15	3
Stream bank – mine	Bank comprised of mine sediments (e.g., dressing waste)	15	3
Channel sediment (mine area)	Exposed within-channel sediments	15	3
Channel sediment (wider catchment)	Exposed within-channel sediments	15 (5 from Garrigill Burn, 5 from S. Tyne u/s of confluence, 5 from S. Tyne d/s of confluence)	3
TOTAL		120	24

Table 2

Soil guideline values for Pb and Zn (after Macklin et al., 2006; Buchman, 2008)

Guidelines	Context	Pb (mg kg^{-1})	Zn (mg kg^{-1})
UK CLEA SGV	Residential with plant uptake	450	-
	Residential without plant uptake	450	-
	Allotments	450	-
	Commercial / industrial	750	-
Dutch soil remediation	Target	85	140
	Intervention	530	720
NOAA (SQuiRTs)	Threshold effects level (TEL)	35	123
	Probable effects level (PEL)	91.3	315

Table 3

XRF and ICP-OES summary statistics for Pb and Zn concentrations (mg kg^{-1})

	Pb (all field data)	Pb (mine area)	Pb (Garrigill Burn – stream sediments)	Pb (South Tyne – upstream of confluence)	Pb (South Tyne – downstream of confluence)	Pb (In situ – lab sample)	Pb (ICP-OES)	Pb (all field data – adjusted)
Mean	5,888	6,481	4,055	220	937	4,774	8,896	11,033
Std. Dev.	10,560	11,092	1,551	38	634	8,506	16,753	20,254
Minimum	61	61	2,126	165	441	61	133	0
Maximum	77,999	77,999	6,638	262	2,189	33,036	75,177	149,340
	Zn (all field data)	Zn (mine area)	Zn (Garrigill Burn – stream sediments)	Zn (South Tyne – upstream of confluence)	Zn (South Tyne – downstream of confluence)	Zn (In situ – lab sample)	Zn (ICP-OES)	Zn (all field data – adjusted)
Mean	2,968	3,057	4,909	160	1,971	2,338	4,092	4,924
Std. Dev.	7,020	7,405	2,748	23	979	3,320	5,331	9,280
Minimum	36	36	1,830	128	471	41	167	1,048
Maximum	69,921	69,921	9,156	185	3,046	14,739	19,358	93,436
Count	120	105	5	5	5	24	24	120

Figure captions:

Fig. 1. Location of Whitesike and Bentyfield mines within the South Tyne catchment. The position of pXRF stream sediment measurements taken along Garrigill Burn and the main River South Tyne are shown in the detail map.

Fig. 2. TLS survey areas and scan positions (A) and XRF sample measurement locations overlain on 1st Edition OS map from 1868 (B) (aerial photograph © Historic England, Historic OS map © Crown Copyright and Landmark Information Group Limited, 2016).

Fig. 3. Sediment budget for the total 18 month TLS monitoring period (September 2012-March 2014) for the combined area at Whitesike and Bentyfield mines. All values in bold are in tonnes. Percentage values indicate the proportion of the total eroded material. N.B. individual storage processes have been combined into overall slope and channel process groupings.

Fig. 4. Surface changes occurring during the period September 2012 – March 2014 at Bentyfield Mine (A), Whitesike Mine (B), and the shared tailings heaps (C).

Fig. 5. Sediment budgets for the separate TLS survey areas at Whitesike and Bentyfield mines and the tailings heaps, representing total recorded net change over the 18 month monitoring period. All values in bold are in tonnes. Percentage values indicate the proportion of the total eroded material. N.B. individual storage processes have been combined into overall slope and channel process groupings.

Fig. 6. Field photographs facing downstream (A) and upstream (B) and UAV aerial image (C) showing the tailings heaps located to the west of Whitesike Mine. The UAV imagery was captured at the start of the TLS monitoring period in September 2012, while the field photographs were taken in March 2014 during the final survey. Garrigill Burn can be seen flowing from right to left (east to west) through a culvert underneath the main tailings heaps.

Fig. 7. Pairwise change detection results between the 14 individual TLS survey dates for the main gully system on the western slope of the tailings heaps. Data are displayed with the viewer positioned face-on and slightly above the slope. Sequence is read from left to right and row by row.

Fig. 8. Relationship between (A) rainfall and daily mean discharge for the River South Tyne at Alston and net volumetric change per day for (B) gullying of the tailings heaps and (C) bank erosion at Whitesike Mine. River South Tyne data are from the UK National River Flow Archive. Error bars are based on the spatially variable change detection analysis conducted at a 95% confidence interval outlined in the methodology.

Fig. 9. Pb and Zn concentration variability for each of the stratified pXRF sample categories. The horizontal lines represent the median value, the length of the box represents the interquartile range (IQR), while the whiskers define all data within 1.5 IQR of the nearer quartile. Data points beyond 1.5 IQR are shown individually.

Fig. 10. Pb (A) and Zn (B) concentrations recorded during the pXRF survey of Whitesike and Bentyfield mines, displayed as modelled (interpolated) surfaces.

Fig. 11. Graphs of downstream variation in Pb (A) and Zn (B) concentrations at Whitesike and Bentyfield mines, based on the results of the field XRF survey. The locations of the key mining features are indicated for reference. The extent of the main mined area relates to the polygon shown on Fig. 10. The right-hand extent of the graph indicates the confluence with the River South Tyne.

Fig. 12. Changes in Pb and Zn values along the main River South Tyne in relation to the confluence with Garrigill Burn.

Fig. 13. Budget diagram showing approximate contaminant flux from the entire mined area for Pb and Zn. Values in bold are in tonnes and percentages relate to the proportion of the total eroded material.

Highlights (85 characters or less)

Contaminated sediment flux was quantified using a novel high resolution methodology.

Erosion was dominated by gullying (60%) and bank erosion (30%).

Slope-channel coupling was high, with the export of 97% of the eroded sediments.

3.1 t a^{-1} of Pb enters the stream, equivalent to 3% of annual 1845-1900 mine output.

Abandoned mines represent persistent sources of contaminated legacy sediments.

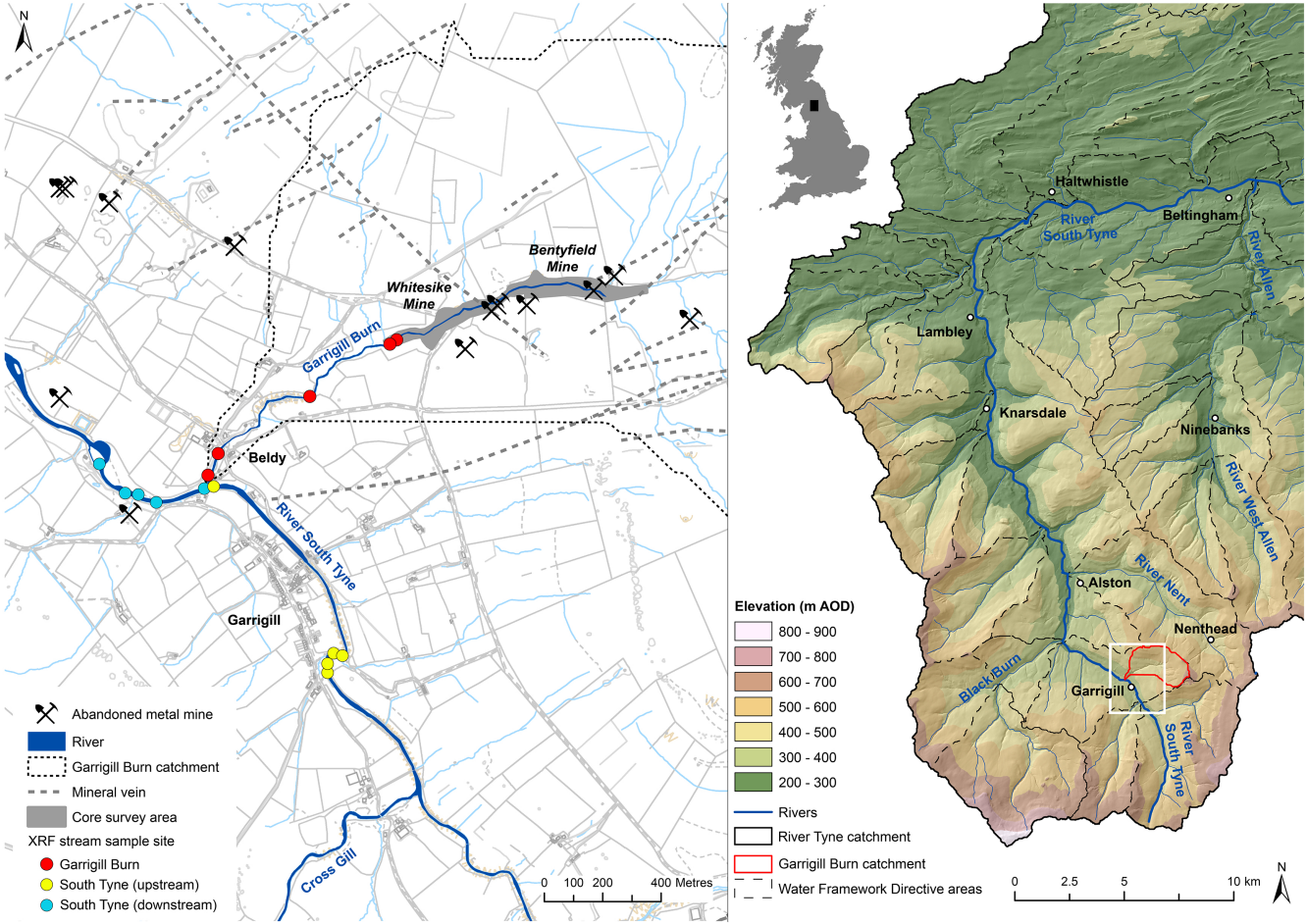
N
Bentyfield Mine
Whitesike Mine
Garrigill Burn
Beldy
River South Tyne
Garrigill
Cross Gill
Abandoned metal mine
River
Garrigill Burn catchment
Mineral vein
Core survey area
XRF stream sample site
Garrigill Burn
South Tyne (upstream)
South Tyne (downstream)
0 100 200 400 Metres
Haltwhistle
Beltingham
River South Tyne
River Allen
Lambley
Knarsdale
Ninebanks
River West Allen
Alston
River Nent
Nenthead
Black Burn
Garrigill
River South Tyne
Elevation (m AOD)
800 - 900
700 - 800
600 - 700
500 - 600
400 - 500
300 - 400
200 - 300
Rivers
River Tyne catchment
Garrigill Burn catchment
Water Framework Directive areas
0 2.5 5 10 km
N

Figure 1

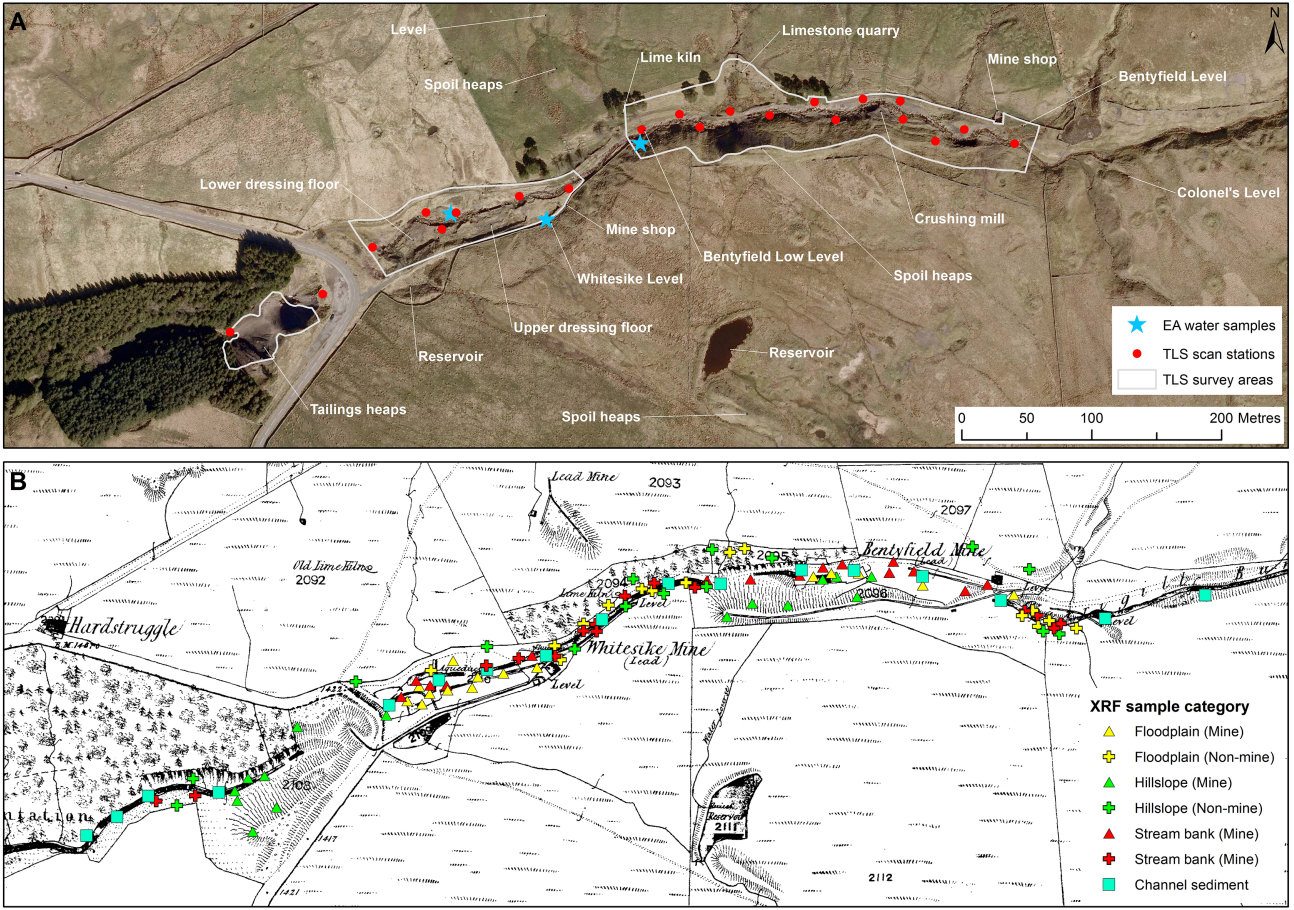
A
Level
Limestone quarry
Lime kiln
Spoil heaps
Mine shop
Bentyfield Level
Lower dressing floor
Colonel's Level
Crushing mill
Mine shop
Bentyfield Low Level
Spoil heaps
Whitesike Level
Upper dressing floor
Reservoir
Reservoir
Tailings heaps
Spoil heaps
N
EA water samples
TLS scan stations
TLS survey areas
0
50
100
200 Metres
B
Lead Mine
2093
2097
Old Lime Kilns
2092
Bentyfield Mine
(Lead)
2095
2094
2096
Hardstruggle
Whitesike Mine
(Lead)
Level
2103
2112
XRF sample category
Floodplain (Mine)
Floodplain (Non-mine)
Hillslope (Mine)
Hillslope (Non-mine)
Stream bank (Mine)
Stream bank (Mine)
Channel sediment

Figure 2

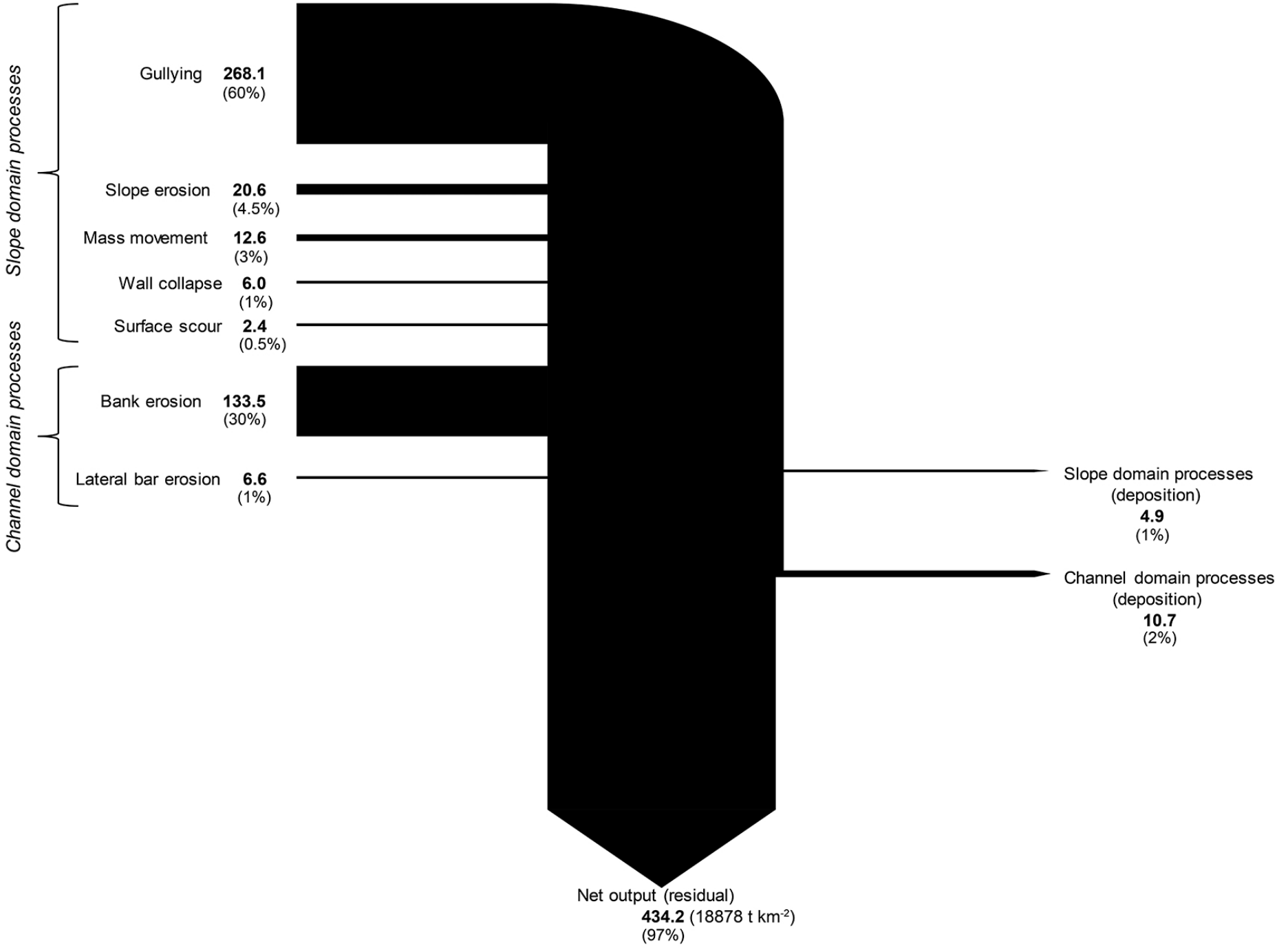
Slope domain processes
Channel domain processes
Gullying 268.1 (60%)
Slope erosion 20.6 (4.5%)
Mass movement 12.6 (3%)
Wall collapse 6.0 (1%)
Surface scour 2.4 (0.5%)
Bank erosion 133.5 (30%)
Lateral bar erosion 6.6 (1%)
Slope domain processes (deposition) 4.9 (1%)
Channel domain processes (deposition) 10.7 (2%)
Net output (residual) 434.2 (18878 t km-2) (97%)

Figure 3

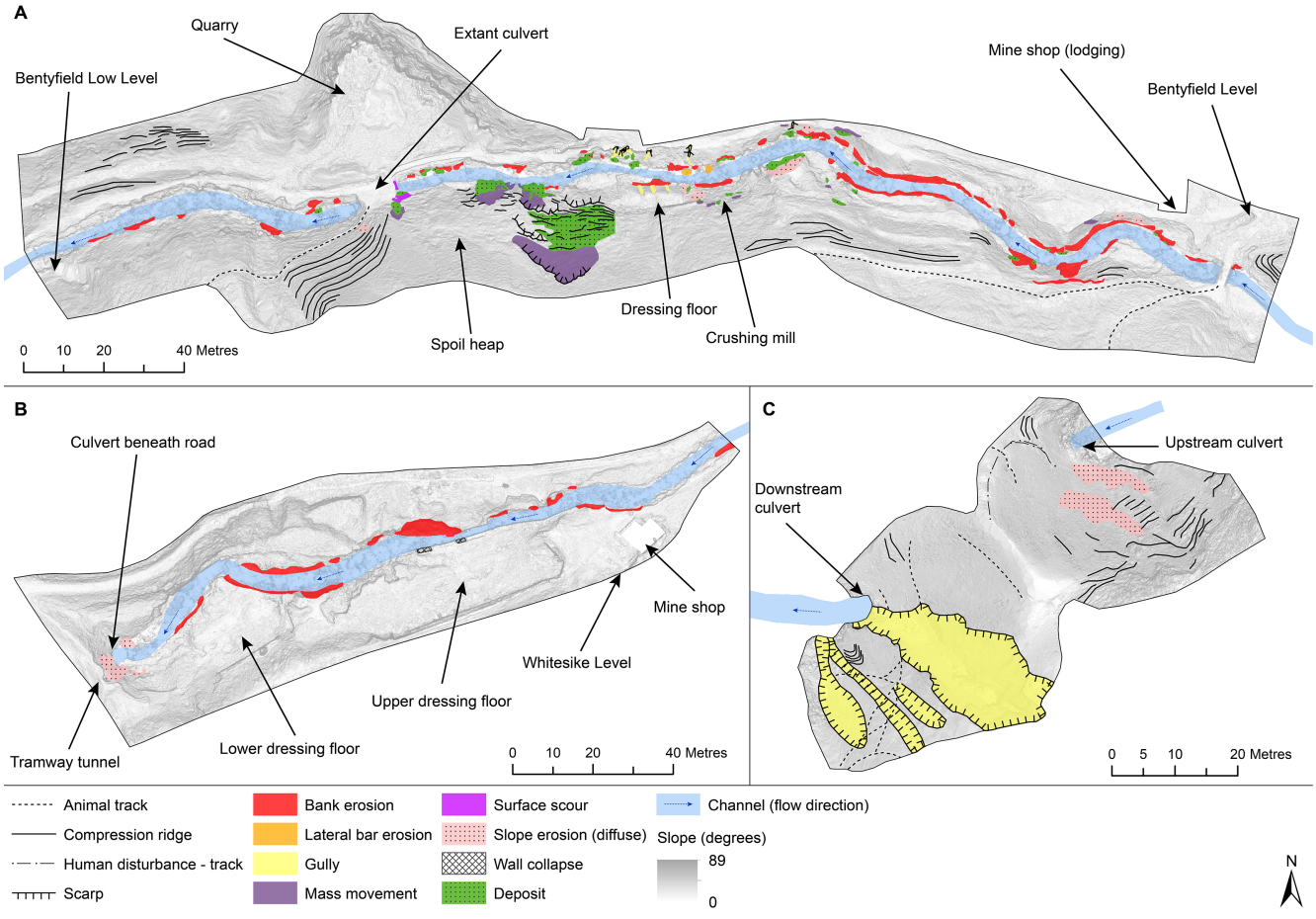
A
Quarry
Extant culvert
Bentyfield Low Level
Mine shop (lodging)
Bentyfield Level
Dressing floor
Crushing mill
Spoil heap
0 10 20 40 Metres
B
Culvert beneath road
Mine shop
Whitesike Level
Upper dressing floor
Lower dressing floor
Tramway tunnel
0 10 20 40 Metres
C
Upstream culvert
Downstream culvert
0 5 10 20 Metres
Animal track
Compression ridge
Human disturbance - track
Scarp
Bank erosion
Lateral bar erosion
Gully
Mass movement
Surface scour
Slope erosion (diffuse)
Wall collapse
Deposit
Channel (flow direction)
Slope (degrees)
89
0
N

Figure 4

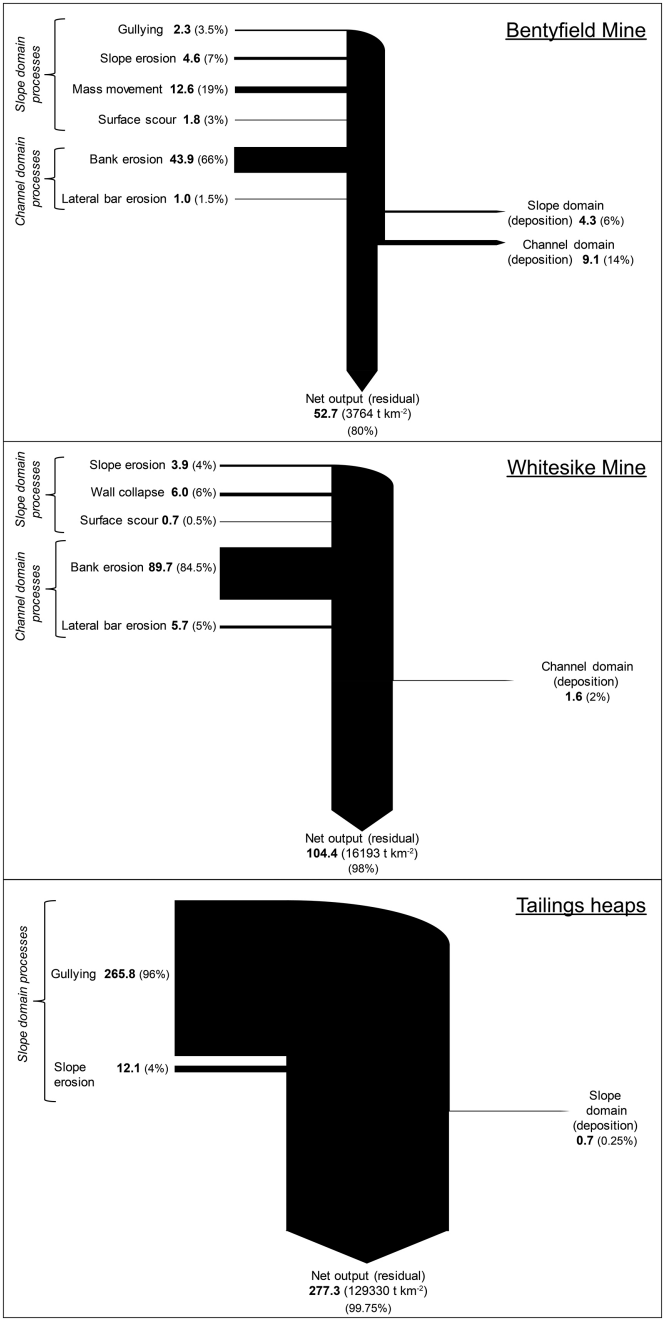
Bentyfield Mine
Slope domain processes
Gullying 2.3 (3.5%)
Slope erosion 4.6 (7%)
Mass movement 12.6 (19%)
Surface scour 1.8 (3%)
Channel domain processes
Bank erosion 43.9 (66%)
Lateral bar erosion 1.0 (1.5%)
Slope domain (deposition) 4.3 (6%)
Channel domain (deposition) 9.1 (14%)
Net output (residual) 52.7 (3764 t km-2) (80%)
Whitesike Mine
Slope domain processes
Slope erosion 3.9 (4%)
Wall collapse 6.0 (6%)
Surface scour 0.7 (0.5%)
Channel domain processes
Bank erosion 89.7 (84.5%)
Lateral bar erosion 5.7 (5%)
Channel domain (deposition) 1.6 (2%)
Net output (residual) 104.4 (16193 t km-2) (98%)
Tailings heaps
Slope domain processes
Gullying 265.8 (96%)
Slope erosion 12.1 (4%)
Slope domain (deposition) 0.7 (0.25%)
Net output (residual) 277.3 (129330 t km-2) (99.75%)

Figure 5

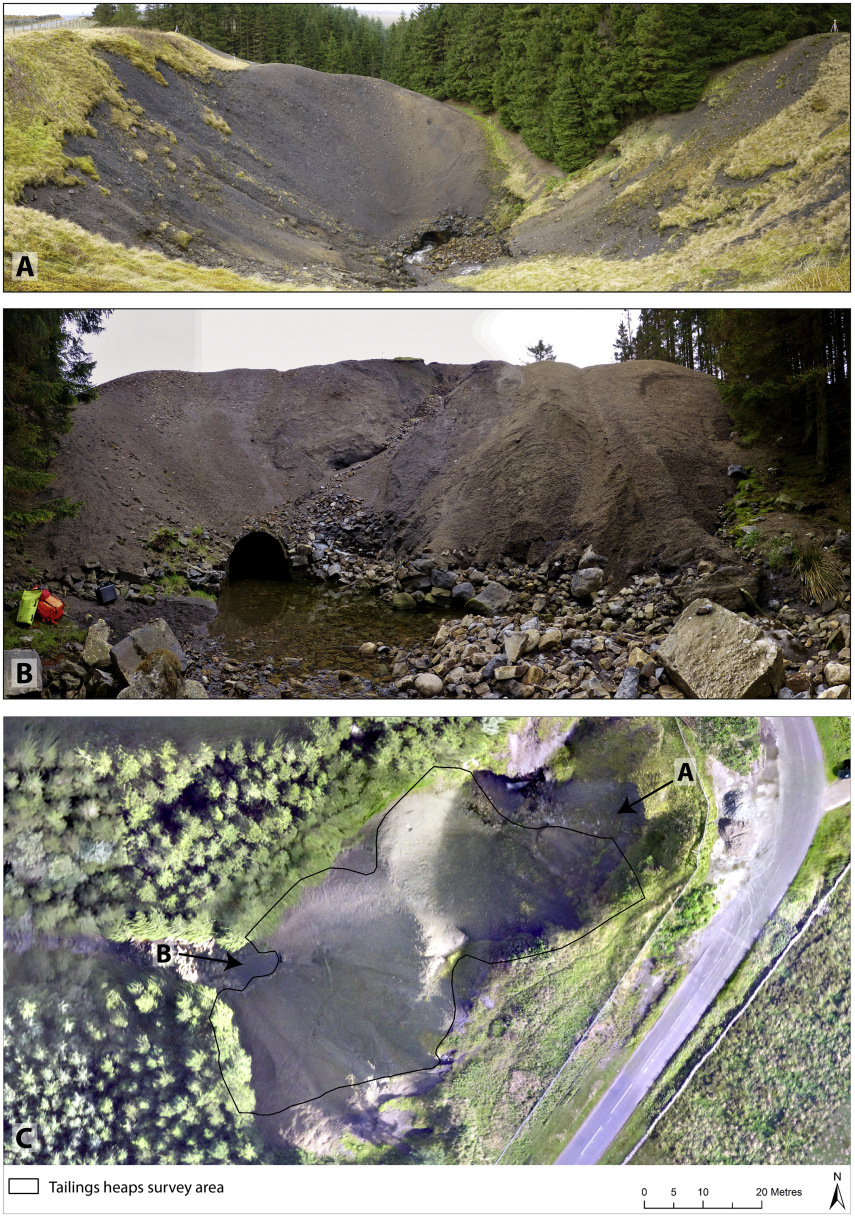

Figure 6

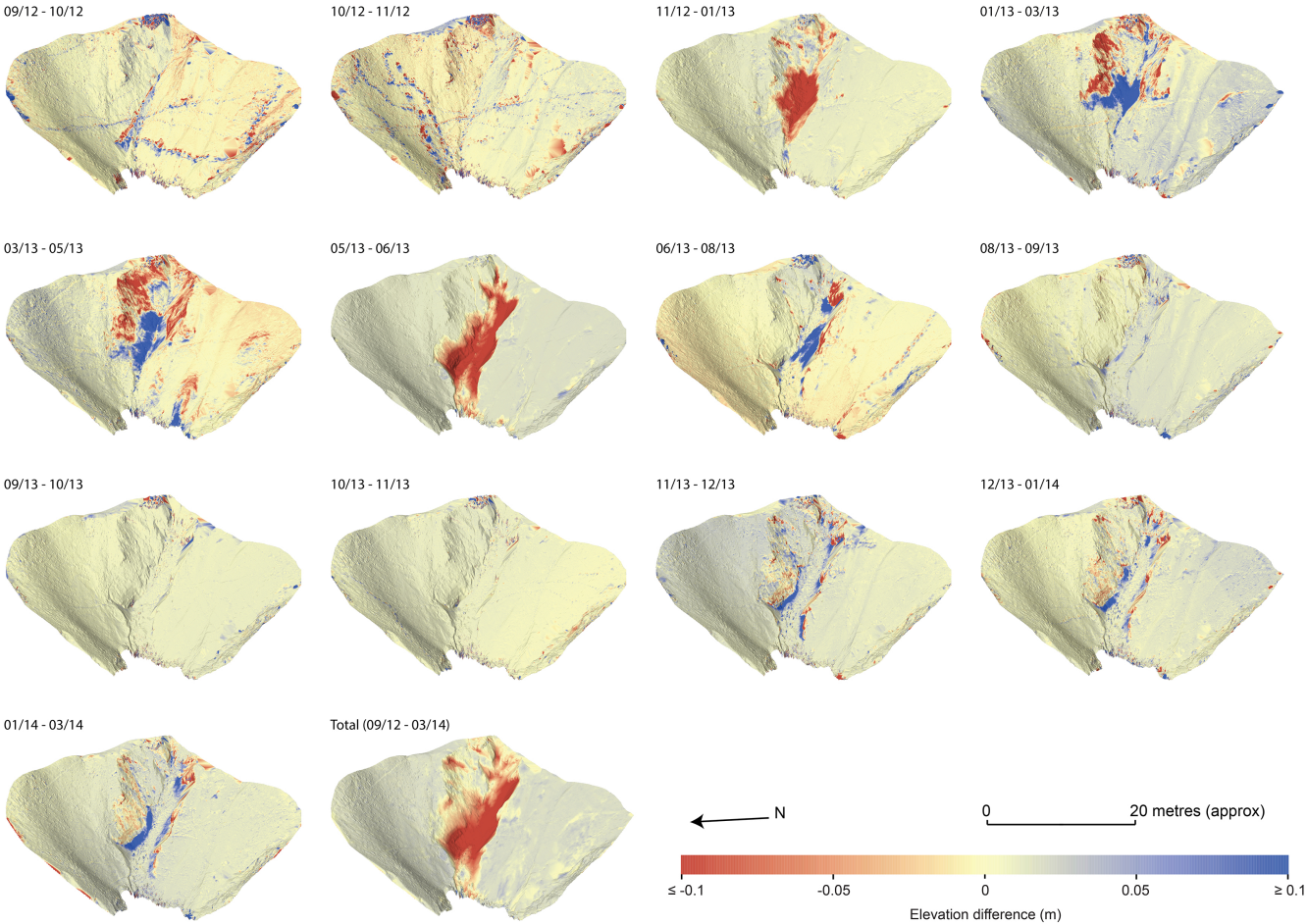
09/12 - 10/12
10/12 - 11/12
11/12 - 01/13
01/13 - 03/13
03/13 - 05/13
05/13 - 06/13
06/13 - 08/13
08/13 - 09/13
09/13 - 10/13
10/13 - 11/13
11/13 - 12/13
12/13 - 01/14
01/14 - 03/14
Total (09/12 - 03/14)
N
0
20 metres (approx)
≤ -0.1
-0.05
0
0.05
≥ 0.1
Elevation difference (m)

Figure 7

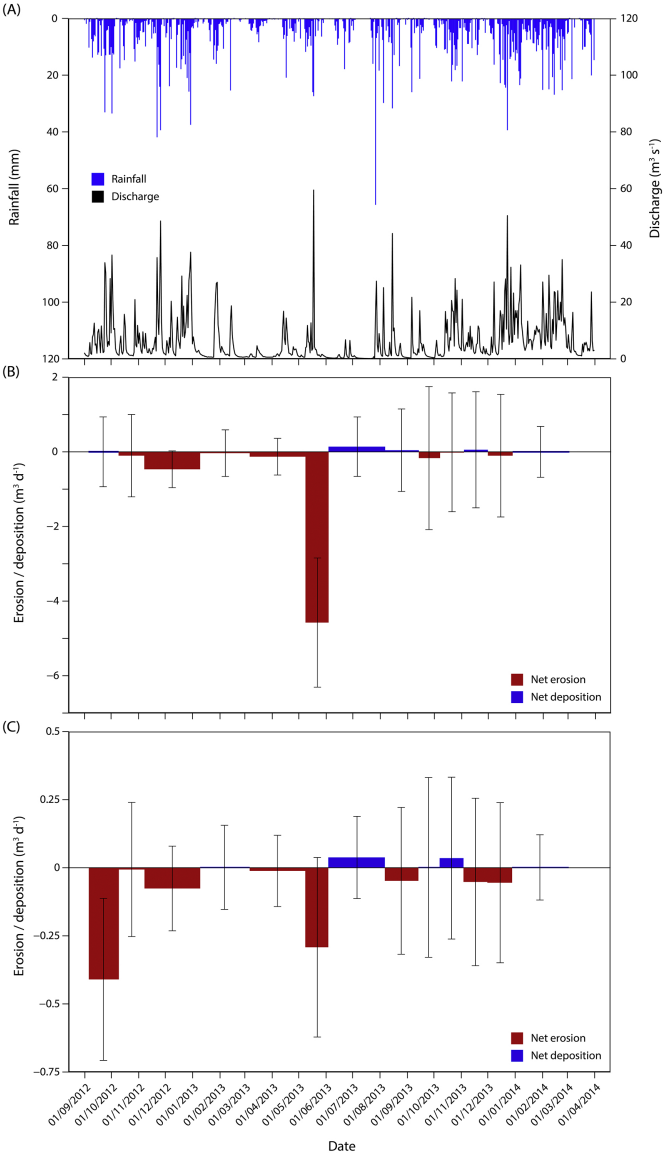
(A)
Rainfall (mm)
Discharge (m³ s⁻¹)
Rainfall
Discharge
(B)
Erosion / deposition (m³ d⁻¹)
Net erosion
Net deposition
(C)
Erosion / deposition (m³ d⁻¹)
Net erosion
Net deposition
01/09/2012
01/10/2012
01/11/2012
01/12/2012
01/01/2013
01/02/2013
01/03/2013
01/04/2013
01/05/2013
01/06/2013
01/07/2013
01/08/2013
01/09/2013
01/10/2013
01/11/2013
01/12/2013
01/01/2014
01/02/2014
01/03/2014
01/04/2014
Date

Figure 8

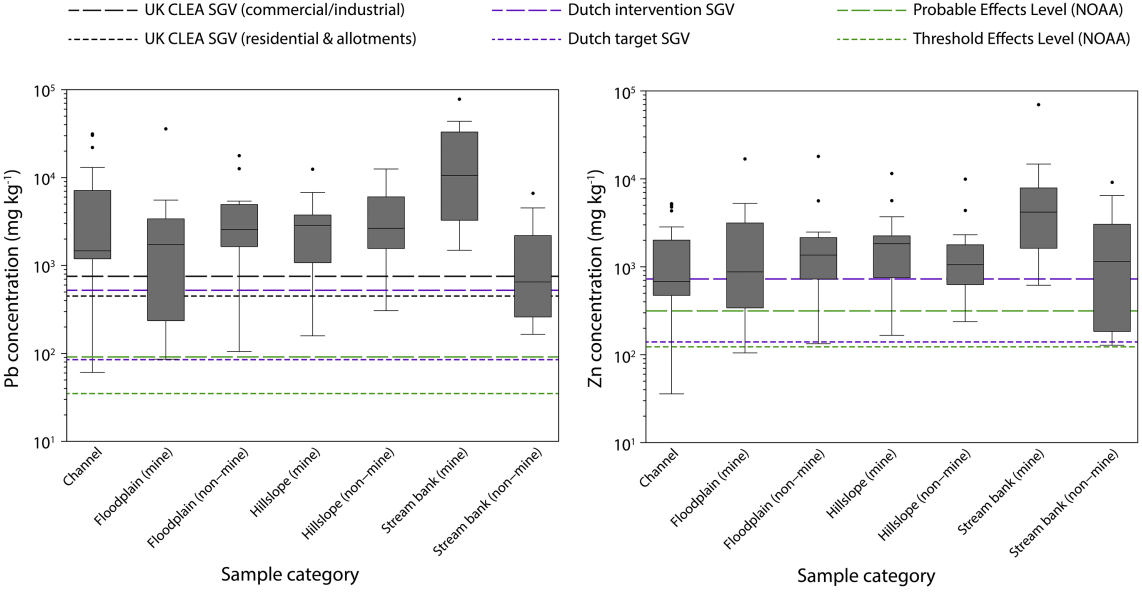
UK CLEA SGV (commercial/industrial)
UK CLEA SGV (residential & allotments)
Dutch intervention SGV
Dutch target SGV
Probable Effects Level (NOAA)
Threshold Effects Level (NOAA)
Pb concentration (mg kg-1)
Zn concentration (mg kg-1)
Channel
Floodplain (mine)
Floodplain (non–mine)
Hillslope (mine)
Hillslope (non–mine)
Stream bank (mine)
Stream bank (non–mine)
Sample category

Figure 9

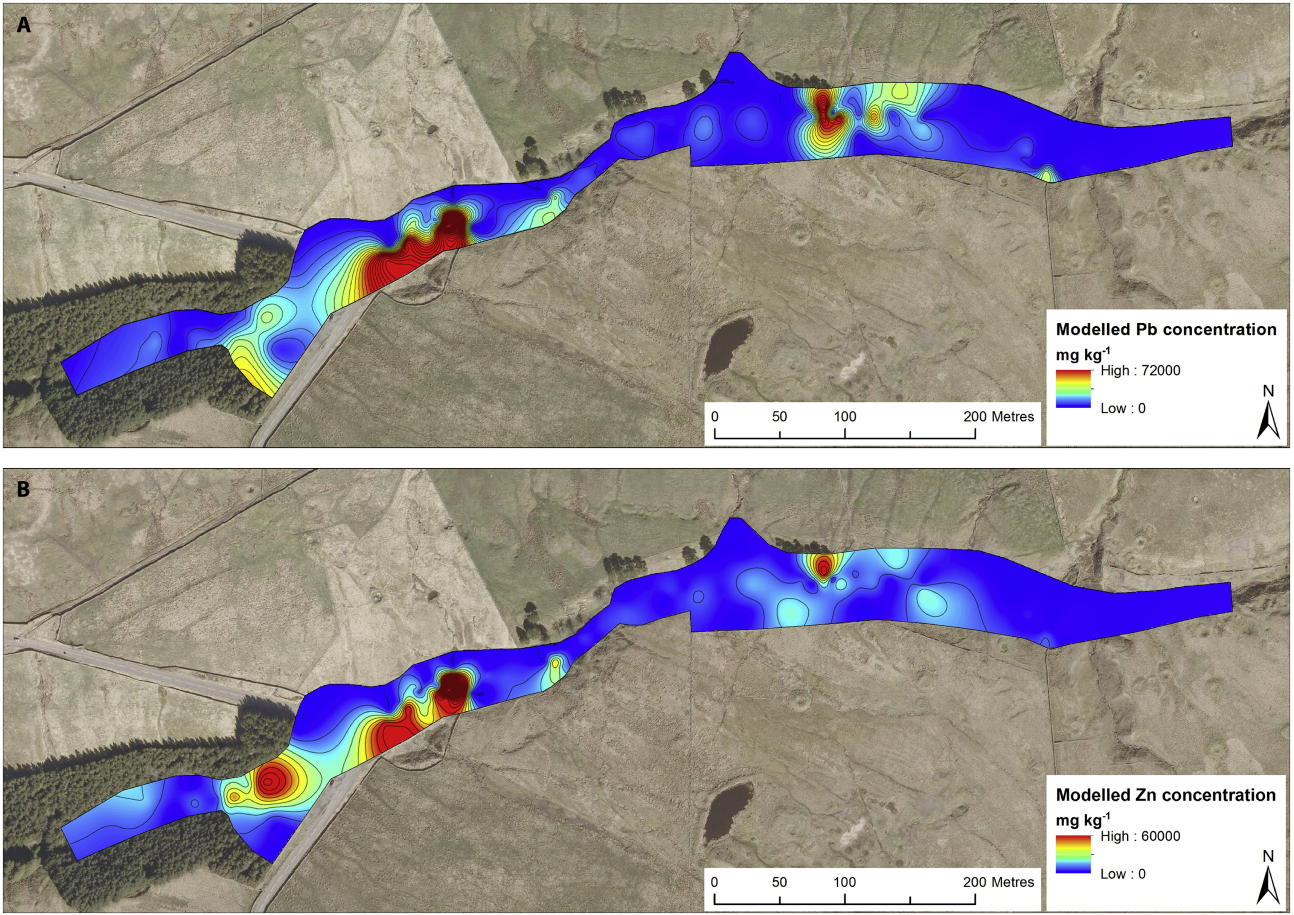
A
Modelled Pb concentration
mg kg-1
High : 72000
Low : 0
N
0 50 100 200 Metres
B
Modelled Zn concentration
mg kg-1
High : 60000
Low : 0
N
0 50 100 200 Metres

Figure 10

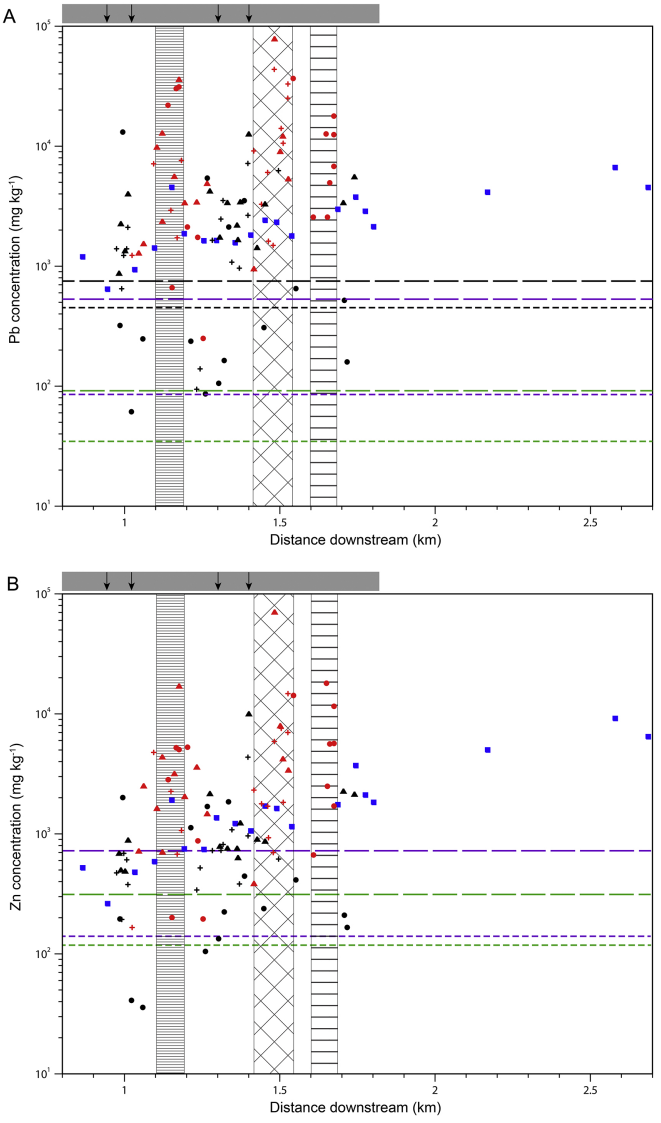
A
Pb concentration (mg kg-1)
Distance downstream (km)
B
Zn concentration (mg kg-1)
Distance downstream (km)
XRF sample categories
Channel sediment
Floodplain sediment (non−mine)
Hillslope sediment (non−mine)
Stream bank sediment (non−mine)
Floodplain sediment (mine)
Hillslope sediment (mine)
Stream bank sediment (mine)
Mining features
Mine level entrances
Bentyfield dressing floor
Whitesike dressing floors
Tailings heaps
Extent of main mined area
Soil guideline values (SGVs)
UK CLEA SGV (commercial/industrial)
UK CLEA SGV (residential & allotments)
Dutch intervention SGV
Dutch target SGV
Probable Effects Level (NOAA)
Threshold Effects Level (NOAA)

Figure 11

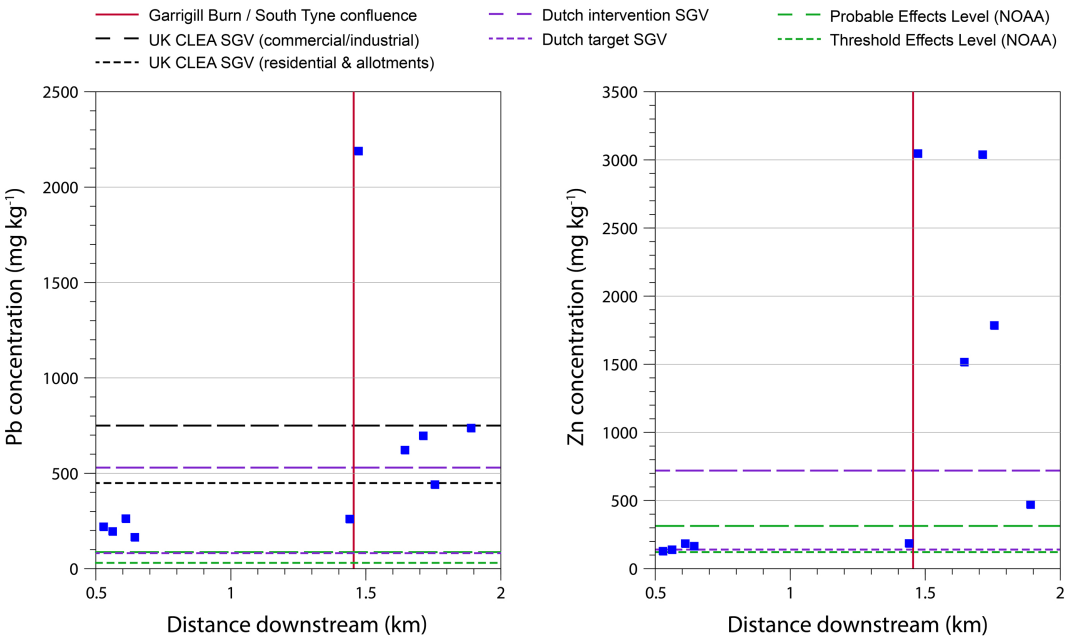
Garrigill Burn / South Tyne confluence
UK CLEA SGV (commercial/industrial)
UK CLEA SGV (residential & allotments)
Dutch intervention SGV
Dutch target SGV
Probable Effects Level (NOAA)
Threshold Effects Level (NOAA)
Pb concentration (mg kg-1)
Zn concentration (mg kg-1)
Distance downstream (km)
Distance downstream (km)

Figure 12

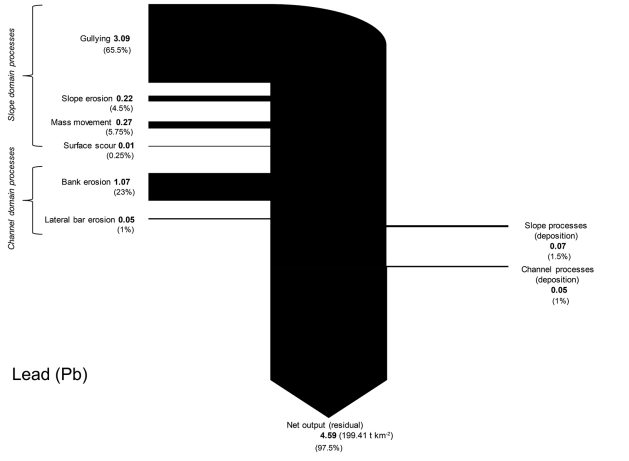
Slope domain processes
Channel domain processes
Gullying 3.09 (65.5%)
Slope erosion 0.22 (4.5%)
Mass movement 0.27 (5.75%)
Surface scour 0.01 (0.25%)
Bank erosion 1.07 (23%)
Lateral bar erosion 0.05 (1%)
Slope processes (deposition) 0.07 (1.5%)
Channel processes (deposition) 0.05 (1%)
Lead (Pb)
Net output (residual) 4.59 (199.41 t km-2) (97.5%)

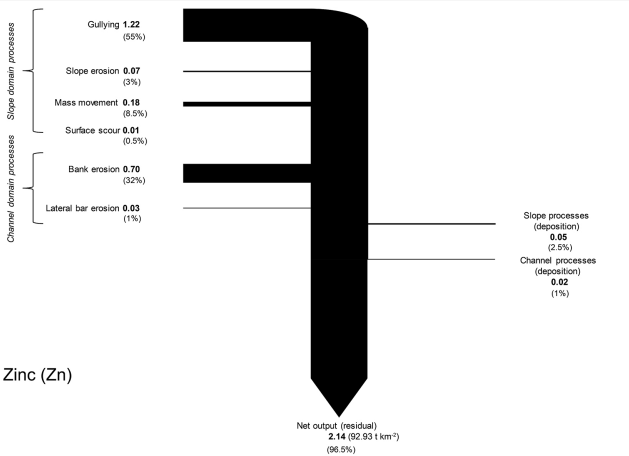
Slope domain processes
Channel domain processes
Gullying 1.22 (55%)
Slope erosion 0.07 (3%)
Mass movement 0.18 (8.5%)
Surface scour 0.01 (0.5%)
Bank erosion 0.70 (32%)
Lateral bar erosion 0.03 (1%)
Slope processes (deposition) 0.05 (2.5%)
Channel processes (deposition) 0.02 (1%)
Zinc (Zn)
Net output (residual) 2.14 (92.93 t km-2) (96.5%)

Figure 13